Pergamon

Geochimica et Cosmochimica Acta, Vol. 66, No. 13, pp. 2379–2397, 2002

0016-7037/02 $22.00 + .00

PII S0016-7037(02)00839-6

An investigation of artificial biasing in detrital zircon U-Pb geochronology due to magnetic separation in sample preparation

KEITH N. SIRCOMBE*,† and RICHARD A. STERN

Continental Geoscience Division, Geological Survey of Canada, 601 Booth St., Ottawa, Ontario, K1A 0E8, Canada

(*Received December* 14, 2001; *accepted in revised form January* 23, 2002)

Abstract—The application of detrital zircon geochronology for provenance analysis is complicated by the presence of biases induced by natural processes and sample preparation. The biasing of age distributions as a result of magnetic susceptibility is illustrated using sensitive high resolution ion microprobe dating of detrital zircon from a metaquartzite sample partitioned using a Frantz magnetic barrier separator. The relationship of paramagnetism with U content, α-dose, and discordance is demonstrated, but no relationship between grain size and discordance or age is found. The data also demonstrate that previous limits of zircon survival in sedimentary processes based on U content alone are too simplistic. Two age modes at ~3150 and ~2960 Ma are present in all the paramagnetic fractions; there is a bias toward the ~3150 Ma mode being more prominent in the least-paramagnetic fractions. While the ~2960 Ma is present in the least-paramagnetic fraction, it is argued that such fortuitous representation cannot be assumed before analysis. Such "there or not" provenance interpretations are considered simplistic, and at the very least there is no harm in broadening the range of paramagnetic fractions sampled for analysis. The results indicate a compromise between broad representation and analytical efficiency (avoiding discordant and thus unreliable results) can be made with a Frantz setting of ~1.8 A and 10° side-slope. *Copyright © 2002 Elsevier Science Ltd*

1. INTRODUCTION

Detrital zircon geochronology for provenance analysis has become an increasingly used method for tectonic and crustal evolution issues (e.g., Dodson et al., 1988; Davis et al., 1994; Rainbird et al., 1998). Like all analytical methodologies, detrital zircon geochronology is subject to a variety of assumptions and limitations. In particular, detrital zircon grains in any sedimentary unit sampled for geochronology have been subject to various natural processes before and during deposition that bias interpretations. These include underrepresentation of source rocks with low zircon content, preferential destruction of metamict grains during transportation, and grain-size sorting during deposition. Artificial biases are induced during multiple levels of sample selection (from collection at the outcrop to crushing and hand picking and even ion probe spot location). These biases preclude the ideal situation of being able to exactly match the quantity of analysed grains with the volume of contributing source rock in a pure quantitative interpretation.

One of the fundamental procedures in zircon U-Pb geochronology is the use of magnetic separation to obtain sample fractions that yield more analyses that are concordant. Concordant detrital zircon ages are clearly more powerful than discordant ages. The positive correlation between Pb-loss/discordance, U content, and magnetic susceptibility was noted by Silver (1963a). Refinements to the magnetic separation techniques and the introduction of air abrasion to minimize discordance were developed by Krogh (1982). Heaman and Parrish (1991) later speculated that the routine selection of grains from the least-magnetic fraction introduced the possibility of an artificial bias in the resulting U-Pb age distribution. Such a bias may be negligible for zircons of generally unimodal origin such as those in most igneous and some metamorphic units. However, it is a major concern in sedimentary units where zircons of diverse origin are typical, and reasonable representation is sought.

The aims of this paper are to (1) review the known causes of zircon magnetic susceptibility and the functioning of the Frantz magnetic barrier separator, (2) examine the potential for biasing in a typical provenance analysis project based on detrital zircon geochronology, and (3) provide some guidelines for researchers conducting similar provenance projects to monitor and/or avoid potential artificial paramagnetic biasing.

2. MAGNETIC SUSCEPTIBILITY OF ZIRCON

The use of the Frantz magnetic barrier separator to fractionate zircon based on paramagnetism or magnetic susceptibility has become so common in geochronology that it barely receives a mention in the modern literature. This section will discuss the features of magnetic susceptibility in zircon relevant to this investigation. A detailed review of the functioning of the Frantz magnetic barrier separator based on these principles is given in the Appendix.

Magnetic susceptibility is the measure of the ease with which a material is magnetized by the application of a magnetic field. This value can be considered in terms of volume magnetic susceptibility (χ_v) or mass magnetic susceptibility (χ_g), which is derived by dividing volume magnetic susceptibility by the density of the material being examined (4.6–4.7 g/cm^3 for zircon; Deer et al., 1992). The density of zircon changes with metamictization up to a saturation level at ~3.9 g/cm^3 or a density decrease of ~17% (Murakami et al., 1991). However, the density change itself is not important in the discussion here,

* Author to whom correspondence should be addressed (ksircombe@tsrc.uwa.edu.au).
† *Present address:* Tectonics Special Research Centre, Department of Geology and Geophysics, University of Western Australia, 35 Stirling Highway, Crawley WA 6009, Australia.

because the Frantz separator fractionates by relative magnetic susceptibility only. Although magnetic susceptibility is in itself dimensionless, in many references, mass magnetic susceptibility is reported in values based on CGS units such as gauss, centimetre, and gram, and this is often indicated by the nomenclature, e.m.u./g. CGS mass magnetic susceptibility can be converted to a value based on SI units by multiplying by $4\pi/1000$ (Payne, 1981). SI-based values are distinguished by m^3/kg. Although by historical necessity the discussion here will use CGS-based values, both values will be included.

There are three magnetic states of matter relevant for this discussion. Diamagnetic materials have negative magnetic susceptibilities and are weakly repelled by a magnetic field. Paramagnetic materials have positive magnetic susceptibilities and are moderately attracted by a magnetic field. Ferromagnetic materials, such as iron and many iron compounds, have high positive magnetic susceptibilities and are strongly attracted by a magnetic field.

The typical value of mass magnetic susceptibility for zircon ranges from diamagnetic to paramagnetic. Lewis and Senftle (1966) calculated from a theoretical basis that pure zirconium orthosilicate ($ZrSiO_4$) is diamagnetic at -0.39×10^{-6} e.m.u./g (-4.9×10^{-9} m^3/kg). They also measured diamagnetic and paramagnetic values for their samples ranging from -0.25×10^{-6} to $+6.6 \times 10^{-6}$ e.m.u./g (-3.1×10^{-9} to 8.3×10^{-8} m^3/kg) with most specimens having susceptibilities $<1 \times 10^{-6}$ e.m.u./g (1.3×10^{-8} m^3/kg). Other reported measurements of mass magnetic susceptibility in zircon range from 0.163×10^{-6} to 0.258×10^{-6} e.m.u./g (2.0×10^{-9} to 3.2×10^{-9} m^3/kg) (Powell and Ballard, 1968). S. G. Frantz in the Appendix of Gaudin and Spedden (1943) reported "negative mass susceptibility in the order of -0.3×10^{-6}" (-3.8×10^{-9} m^3/kg). The possibility of anisotropic magnetic susceptibility in zircon was raised by measurements of Voigt and Kinoshita (1907): -0.170×10^{-6} e.m.u./g (-2.14×10^{-9} m^3/kg) $\|$ a-axis, and 0.732×10^{-6} e.m.u./g (9.20×10^{-9} m^3/kg) $\|$ c-axis. These anisotropic values have since been repeated in Landolt-Börnstein tables, although the original analysts appear to have used an impure zircon sample and stated that they considered the values to have low reliability.

The actual cause of magnetic susceptibility in zircon has only been briefly examined. Using a series of leaching and heating/oxidizing experiments Lewis and Senftle (1966) demonstrated the cause to be the combination of a readily soluble but unidentified mineral on the zircon surface and iron impurities in the crystal lattice. Lewis and Senftle (1966) also discussed the metamictization of the zircon-enhancing diffusion of iron from external sources, such as groundwater, into the crystal lattice.

3. SAMPLE DESCRIPTION

The sample used in this study is from the Slave craton, Northwest Territories, Canada, and forms part of a Mesoarchean metasedimentary succession that has been extensively studied in the region (Bleeker et al., 1999; Isachsen and Bowring, 1997). The sample had been previously analysed as part of a regional provenance project (Sircombe et al., 2001) that tested and established a regional correlation across lithostratigraphically similar, but widely dispersed, metasedimentary units. The sample was selected because of our familiarity with the location and the provenance issues involved. The previously analysed age distribution contains a broad range of ages, and in particular, two distinct modes that were considered a suitable target to test for provenance biasing. Previous investigations in the area have also provided a geochronologic constraint from overlying volcanics. Finally, the sample had also previously yielded a couple of grains older than 3800 Ma. Because the search for such ancient grains is of particular interest in many studies of Precambrian sedimentary rocks, there was also a desire to understand how the presence of these ancient grains related to magnetic susceptibility.

The sample is a white-to-green fuchsitic metaquartzite sampled on the south shore of Dwyer Lake, ~30 km north of Yellowknife. The quartzite succession overlies ~2900 Ma or older basement granitoids (Isachsen and Bowring, 1997). Remnant decimetre-scale cross-beds are preserved at the sample locality, commonly outlined by fuchsitic (± relict detrital chromite) laminae. The quartzite is overlain by a thin felsic volcanic-to-volcaniclastic unit dated at 2853 $+2/-1$ Ma (Ketchum and Bleeker, 2000), which in turn is overlain by BIF and the main volcanic succession of the Yellowknife greenstone belt.

The age distribution in the sample spans one billion years and includes two principal age modes. The first is a ~2960 Ma component and is correlated with a widespread plutonic event in the Central Slave Basement Complex involving the intrusion of tonalites, i.e., Event VII in the nomenclature of Bleeker and Davis (1999). The second component is ~3150 Ma and is correlated with plutonic-metamorphic event in the same basement complex involving the intrusion of tonalites to granites and their deformation (Event V: Bleeker and Davis, 1999). A range of older ages with no distinct mode occur up to 3900 Ma.

4. ANALYTICAL METHODOLOGY

Detrital zircon grains were extracted using standard crushing, milling, Wilfley table, and heavy liquid techniques. Five fractions were separated using the Frantz magnetic barrier separator at the settings shown in Table 1 after removing ferromagnetic minerals with a hand-magnet. The range of mass magnetic susceptibilities represented by each fraction, from A, the least paramagnetic, to E, the most paramagnetic, is illustrated in Figure 1. Ideally, the absolute mass magnetic susceptibility should be used when describing paramagnetic fractions. The theoretical relationship between these values and the settings on a Frantz is discussed in the Appendix with an example of direct calibration. However, it must be acknowledged that this relationship probably varies to some extent between separators, and the significance of this variation remains to be investigated. For the purposes of this study, it is assumed that the performance of the Frantz used matches the theoretical calculations.

The handpicking process in detrital zircon geochronology attempts to ensure the most-representative sampling possible within the limitations imposed by handling small-sized samples. No preferential selection of zircon was made based on size, color, shape, roundness, and metamictization. This aim is best achieved by minimising individual grain handling and hand picking only to ensure purity of zircon content as a group rather than the quality of individual grains. Extracted zircon grains were poured into a mound under alcohol in a Petri dish. This mound was directly mixed and then a swathe swept from the middle. Non-zircon grains were removed from this swathe, and the remaining zircon grains, typically numbering 100 to 150 grains, were taken from the dish using a pipette. Zircon grains were mounted on double-sided adhesive tape before being set in an epoxy disk and polished to reveal half-sections. Zircon internal structures were analysed and interpreted from backscattered electron imaging. During analysis, an array of mounted zircon grains was systematically analysed with the only

Table 1. Frantz settings and calculated mass magnetic susceptibility values used in this study.

Setting	$\theta°$ side-slope	i A amps	$H{\cdot}dH/dx$ "Gauss^2/cm"†	χ_g cgs "emu/g"	χ_g SI "m^3/kg"	Fraction§
1	5	0.5	3.74×10^7	2.28×10^{-6}	2.87×10^{-8}	E
2	10	1.0	2.21×10^8	7.69×10^{-7}	9.66×10^{-9}	D
3	10	1.8	3.60×10^8	4.72×10^{-7}	9.66×10^{-9}	C
4	5	1.8	3.60×10^8	2.37×10^{-7}	2.98×10^{-9}	B
5	1	1.8	3.60×10^8	4.75×10^{-8}	5.96×10^{-10}	A

† Magnetic energy gradient strength values obtained from documentation supplied by S.G. Frantz Company Inc. and discussed in Appendix.
§ Fraction identification next to upper bound of magnetic susceptibility range, i.e. fraction E comprises grains ranging from 2.87×10^{-8} to 9.66×10^{-9} (m^3/kg). Grains in fraction A potentially range from 5.96×10^{-10} to a theoretically pure zircon diamagnetic value -4.9×10^{-9} (m^3/kg) Lewis and Senftle, 1966.

operator choice being the avoidance of any obvious imperfections in the grain surfaces.

Because grain size is a frequent consideration in conventional zircon analysis (Silver, 1963b; Silver and Deutsch, 1963) and a potential provenance feature (Morton et al., 1996), the sizes of analysed grains were also measured using digital image analysis. This approach assumes that the 2-D section of a grain is an accurate measurement of the overall size of that grain. Because zircon grains are typically elongate (with mean breadth/length ratio typically 0.6–0.7), three measurements are reported here: breadth, length, and equivalent diameter. The latter is the diameter of a circle of equivalent area as the digitized grain image (Russ, 1994). This measurement better reflects the potential hydraulic behavior of the grain than breadth alone. Breadth reflects the equivalent sieve mesh size and is thus compatible with conventional sedimentological grain-size measurements. The sorting and skewness parameters described here have been calculated using standard grain-size statistical procedures (Folk and Ward, 1957; Folk, 1980; Boggs, 1995).

Using standard analytical techniques on the Geological Survey of Canada's SHRIMP II ion microprobe (Stern, 1997), Pb/Pb ratios were measured directly and Pb/U ratios by comparison with known standards (BR266, ^{206}Pb/^{238}U: 0.09059; Kipawa, ^{206}Pb/^{238}U: 0.16654) analysed sequentially with the unknown samples. As described above, at least 60 individual grain analyses are required to satisfy statistical adequacy for detrital investigations (Dodson et al., 1988; Sircombe, 2000a). To reach such a target for all five fractions within a reasonable schedule, the number of scans per analysis was reduced to three. While this has resulted in poorer precision in the age measurements (median $\pm$1 s.e. in the five fractions range from 47–117 Ma) the results remain adequate to test for any age component bias between paramagnetic fractions. Analyses were corrected for common Pb content using ^{204}Pb measurements and examined for concordance/discordance. Because one purpose of this study was to examine compositional correlations with magnetic susceptibility, the otherwise routine canceling of analyses with high ^{204}Pb was avoided. Nevertheless, only measurements with between 5% and -5% discordance have been utilized for subsequent provenance interpretation. Because analyses with extremely high common-Pb and U content have been included, average values may be skewed high. To avoid this, median compositional values are reported.

Grain ages are calculated using the ^{207}Pb/^{206}Pb ratios and reported with errors at $\pm$2 s.e. In the cases where multiple analyses have been made on a single grain, statistically similar ages were pooled, whereas significantly different ages, for instance those associated with rims and cores in electron imaging, were treated as separate provenance ages. Mixture modeling procedures (Sambridge and Compston, 1994) were also applied to deconvolve complex age distributions.

α-dosage values based on U and Th content and age were calculated using the procedures of Murakami et al. (1991) and are used as the basis for quantifying metamictization.

Isotopic, grain-size, and α-dosage data are presented in supplementary tables. Univariate age data are displayed using a combination of histograms and probability/density distributions created by accumulating individual gaussian distributions (Fig. 2) (Sircombe, 2000b).

5. RESULTS

5.1. Previous Analysis: 1.8 A, 5° Non-Magnetic

In the previous examination of this sample (Sircombe et al., 2001), detrital zircon was extracted at the "typical" level as the non-magnetic fraction at an electromagnet current of 1.8 A and 5° side-slope. Grains were analysed with five mass scans. A total of 88 analyses were made on 80 individual grains, yielding 68 concordant ages. The majority of grains have a generally clear appearance and few inclusions. U and common-Pb content have median values of 148 ppm and 3 ppb, respectively, with an average discordance of 2.2%. The concordant ^{207}Pb/^{206}Pb ages can be subdivided broadly into three groups: (1) ~2960 Ma (29% of total concordant grains), (2) ~3150 Ma (34% of total concordant grains), and (3) a broad range between

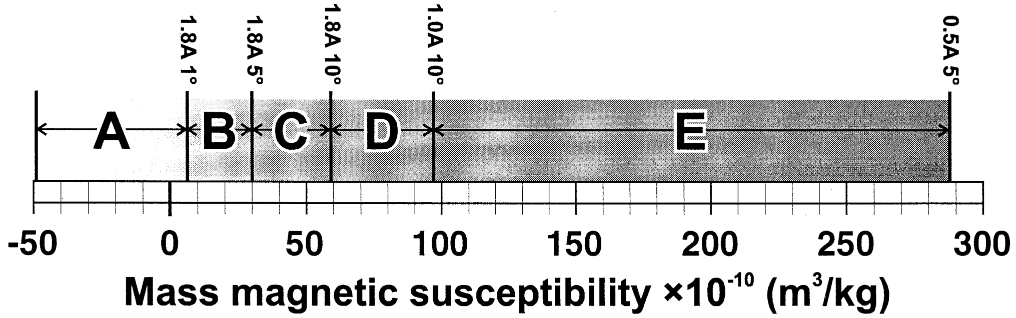

Fig. 1. Illustration of the potential range of mass magnetic susceptibilities represented by the five fractions used in this study ranging from A, the least paramagnetic and potentially also diamagnetic, to E the most paramagnetic. Magnetic susceptibility values as calculated in the Appendix and given in Table 1.

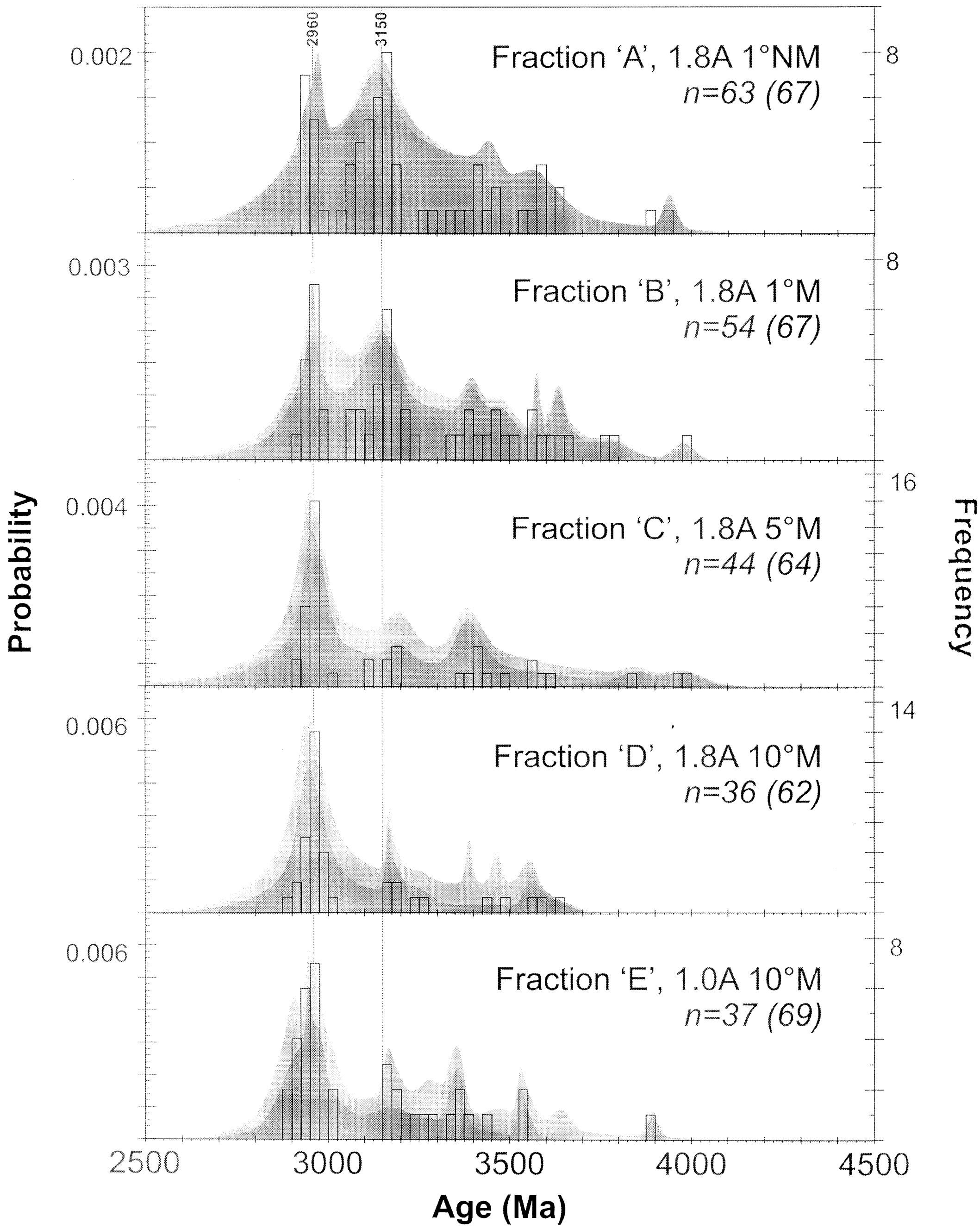

Fig. 2. Age probability density distributions and histograms for the five paramagnetic fractions. Dark-grey-filled curves represent the accumulation of concordant $^{207}Pb/^{206}Pb$ ages scaled to total 1. Light-grey-filled curves represent the combination of concordant and discordant analyses. n = indicates number of concordant ages (between −5 and +5% discordance); (n) indicates total number of analyses.

3300 and 3600 Ma (26% of total concordant grains). The oldest analysed grain is at 3918 ± 10 Ma. Mixture modeling subdivides these groups into several smaller subgroups (Table 2).

5.2. Fraction E: 1.0 A, 10° Paramagnetic

A total of 69 analyses on 68 grains were made, yielding 37 concordant ages. Almost all grains are cloudy and mottled in appearance with common inclusions and corroded surface texture. U and common-Pb content have median values of 714 ppm and 54 ppb, respectively, with an average discordance of 11.7%. The concordant $^{207}Pb/^{206}Pb$ ages are dominated (57%) by an age mode, as defined by mixture modeling, at 2950 ± 10 Ma (Table 2). Two smaller modes occur at 3183 ± 76 Ma (14%) and 3351 ± 17 Ma (19%). Ages ranging between 3300 and 4000 Ma comprise 22% of the total with one age older than 3800 Ma.

Table 2. Summary of mixture modeling age components, grain-size and compositional data.

Previous Dwyer Lake†	Fraction A	Fraction B	Fraction C	Fraction D	Fraction E	Event‡
2945 ± 13 (3)				2949 ± 17 (24)	2950 ± 10 (22)	**VII**
2962 ± 4 (15)	2960 ± 17 (17)	2958 ± 13 (14)	2959 ± 16 (25)			
3042 ± 21 (3)						
3111 ± 11 (8)						**VI**
	3131 ± 34 (26)					
3146 ± 8 (10)		3148 ± 11 (20)				
						V
				3170 ± 13 (6)		
3180 ± 11 (5)			3193 ± 56 (4)		3183 ± 76 (5)	
						IV
various	3305 ± 80 (4)					
individual grains		3398 ± 36 (6)	3392 ± 30 (12)		3351 ± 16 (7)	**III**
	3439 ± 42 (8)	3475 ± 55 (4)				
	3570 ± 62 (6)	3586 ± 5 (4)		3564 ± 26 (5)		II
		3637 ± 26 (3)				
0.29	0.25	0.27	0.26	0.24	0.21	**Sorting ϕ**
0.09	−0.12	−0.12	−0.10	0.05	−0.03	**Skewness**
66 ± 29	56 ± 29	66 ± 29	72 ± 29	69 ± 29	70 ± 29	**Breadth μm**
148	96	181	317	457	714	**U ppm**
3	17	12	16	39	54	**^{204}Pb ppb**
2.2	0.1	4.4	5.6	6.0	11.7	**Discordance**

All age values given with ±2 standard errors. The number of individual analyses (n) assigned to the modeled age component is given in brackets. Note that each sample will have several analyses that are independent of these modeled groups and thus will not be accounted for in the table. U ppm and ^{204}Pb ppb values are median values for each fraction. Discordance is the average percentage value of each fraction. † Data from original analysis of Dwyer Lake quartzite sample Sircombe et al., 2001. ‡ Data are placed in the context of Slave province crustal formation/reworking events defined by Bleeker and Davis, 1999.

5.3. Fraction D: 1.8 A, 10° Paramagnetic

A total of 62 grains were analysed, yielding 36 concordant ages. The appearance of the grains ranges from cloudy to clear with infrequent inclusions and rare corroded surface textures. U and common-Pb content have median values of 457 ppm and 39 ppb, respectively, with an average discordance of 6.0%. The concordant ^{207}Pb/^{206}Pb ages are dominated (67%) by a mode defined by mixture modeling at 2949 ± 17 Ma (Table 2). Two smaller modes occur at 3170 ± 13 Ma (17%) and 3564 ± 26 Ma (14%). Ages ranging between 3300 and 4000 Ma comprise 14% of the total with no ages older than 3800 Ma.

5.4. Fraction C: 1.8 A, 5° Paramagnetic

A total of 64 analyses on 63 individual grains were made, yielding 44 concordant ages. Grains are generally clear in appearance with infrequent inclusions. U and common-Pb content have median values of 317 ppm and 16 ppb, respectively, with an average discordance of 5.6%. The concordant ^{207}Pb/^{206}Pb ages are dominated (57%) by a mode defined by mixture modeling at 2959 ± 16 Ma (Table 2). Two smaller modes occur at 3193 ± 56 Ma (9%) and 3391 ± 30 Ma (27%). Ages ranging between 3300 and 4000 Ma comprise 31% of the total, including three ages older than 3800 Ma.

5.5. Fraction B: 1.8 A, 1° Paramagnetic

A total of 67 analyses on 66 individual grains yielded 54 concordant ages. Grains generally have a clear appearance, infrequent inclusions, and rare overgrowths. U and common-Pb content have median values of 181 ppm and 12 ppb, respectively, with an average discordance of 4.4%. The concordant ^{207}Pb/^{206}Pb ages are dominated by two principal modes at 3148 ± 21 Ma (37%) and 2958 ± 13 Ma (26%) (Table 2). Other minor modes occur in the range from 3300 to 4000 Ma and comprise 37% of the total. The oldest age within all five fractions occurs within this latter fraction at 3979 ± 58 Ma (#B25.1).

5.6. Fraction A: 1.8 A, 1° Non-Magnetic

A total of 67 analyses on 65 individual grains yielded 63 concordant ages. The appearance of the grains is generally very clear with rare inclusions and rare preservation of euhedral crystal faces. U and common-Pb content have median values of 96 ppm and 17 ppb, respectively, with an average discordance of 0.1%. The concordant ^{207}Pb/^{206}Pb ages are dominated by two principal modes at 3131 ± 34 Ma (41%) and 2960 ± 17 Ma (27%) (Table 2). Other minor modes occur in the range from 3300 to 4000 Ma and comprise 29% of the total, including two individual grain ages greater than 3800 Ma.

6. DISCUSSION

6.1. Age Modes, Magnetic Susceptibility, and Metamictization

The most striking feature of this set of data is the presence or absence of grain ages associated with the ~3150 Ma component previously identified (Sircombe et al., 2001). While ages associated with the ~2960 Ma component are ubiquitous in all

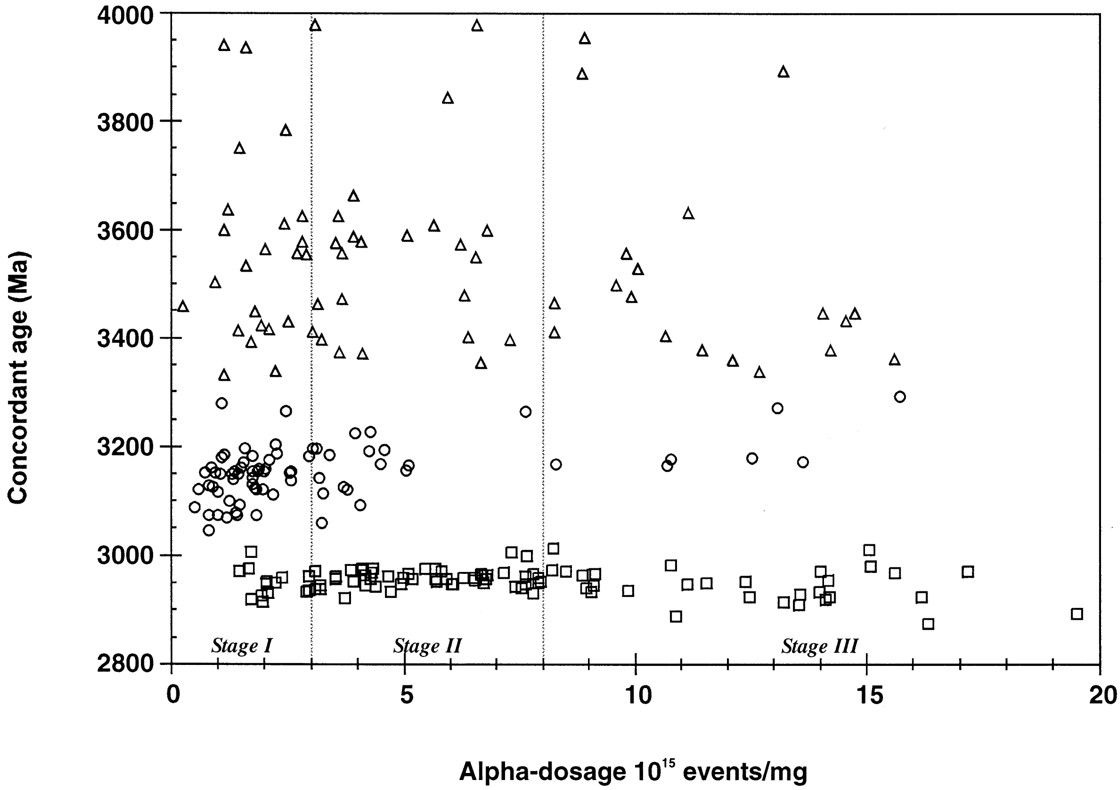

Fig. 3. Scatterplot illustrating the relationship between α-dosage/metamictization and age in the concordant results in the entire set of data. Vertical lines indicate the three divisions of metamictization defined by Murakami et al. (1991) from purely crystalline to highly metamict. Squares, circles, and triangles highlight the ages in the ~2960 Ma, ~3150 Ma, and >3300 Ma age components, respectively.

five fractions, ~3150 Ma ages are only seen prominently in the two least-paramagnetic fractions (Fig. 2). The numerical ratio of ~2960 Ma ages to ~3150 Ma ages varies markedly from 0.41 to 0.70 in fractions A and B, to 3.29, 4.33, and 2.63 in fractions C, D, and E, respectively. The magnetic susceptibility fractionation of the sample clearly influences the presence of zircon grains associated with the ~3150 Ma component. Another feature of the age distributions is the reduction in grains in the >3300 Ma range from 29, 35, and 32% in fractions A, B, and C, respectively, to 14 and 21% in fractions D and E, respectively.

The explanation of these age distribution features lies in the correlations between metamictization, magnetic susceptibility, and age. When concordant ages are plotted against α-dose (Fig. 3), it can be seen that, overall, the ~3150 Ma ages have distinctly lower α-doses than the ~2960 Ma ages, with median values of 2.0 and 6.5×10^{15} α-decay events/mg, respectively.

The correlations between magnetic susceptibility, U content, and discordance, as discussed by Silver (1963a) and Krogh (1982), are further illustrated in this study by Figure 4. The median U content increases with increasing magnetic susceptibility from fraction A to E. Coincident with increased U content is the greater potential for crystal lattice damage as quantified by α-dose (Fig. 4b). The positive correlation between paramagnetism and discordance seen in Figure 4c is consistent with the previous results. These results reinforce the ideas of Lewis and Senftle (1966) that metamictization and the subsequent introduction of Fe-compounds into the zircon lattice contributed to paramagnetism.

6.2. Management of Discordant Results and Paramagnetism

Managing discordant results has long been a major concern of zircon geochronology. Indeed, avoiding discordance is the purpose of the development and continuing wide use of magnetic separation techniques. The relationship between magnetic susceptibility and discordance is further illustrated in this study in which many results, particularly those in the two most-magnetic fractions, are classified as discordant with unreliable age interpretations. Such discordant analyses are routinely excluded from further interpretation—but does this in itself introduce a bias?

Undoubtedly, some biasing does occur. The discordant analyses are more likely to be from the more paramagnetic grains, as shown in Figure 4c. Given sufficient time between formation and transportation, these grains have already been subject to natural biasing because of preferential destruction during transportation. Assuming a representative selection of available grains during hand picking, artificial biasing against discordant grains occurs in two stages. First, although the SHRIMP ion probe increases the range of material that can be analysed, spot location is not truly random because of limitations imposed by internal structures and the avoidance of obvious surface imper-

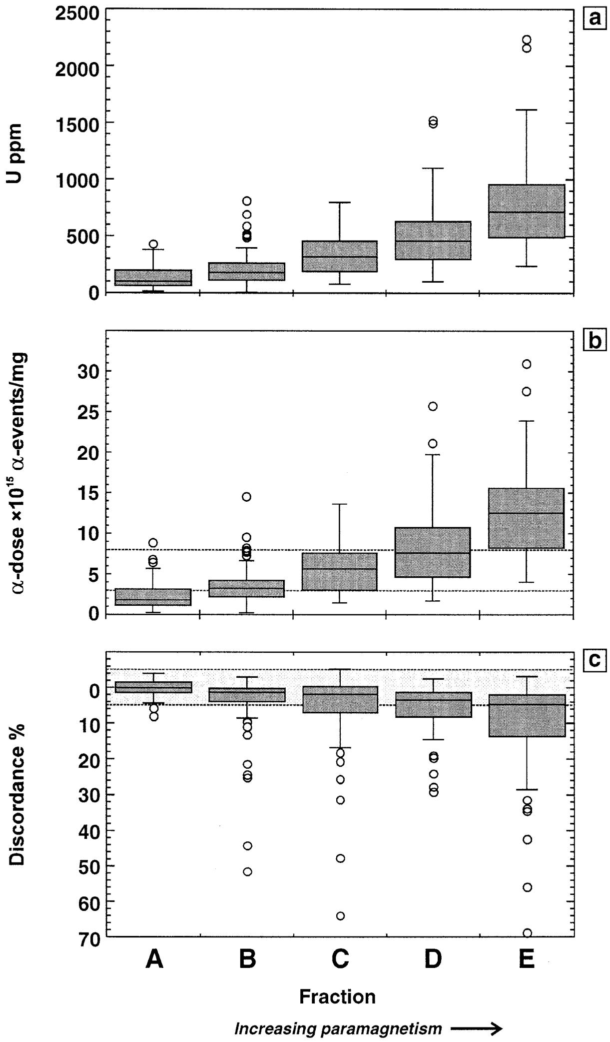

Fig. 4. Box diagrams illustrating the relationships between (a) U content and magnetic susceptibility, (b) α-dosage and magnetic susceptibility, with horizontal lines indicating the metamict stages defined by Murakami et al. (1991), and (c) discordance and magnetic susceptibility represented by the five paramagnetic fractions. All data are included. Boxes represent 50% of the data between the lower and upper quartiles. Circles represent outliers defined as being greater or less than the upper quartile plus 1.5 times the interquartile distance.

fections and/or areas of metamictization. In these cases, it is more important to use the spatial ability of the SHRIMP technique to gain some insight into the age and history of the grain rather than arbitrarily analysing a random spot. The impact of spot selection biasing is considered minimal, because at least part of the grain is still being analysed and is available for interpretation.

The second stage of biasing is the exclusion of results with a particular level of discordance. Quantifying this discard bias is difficult because by definition, the results discarded are unreliable, and, therefore, comparisons between complete and edited data are equally unreliable. However, the results presented here do provide some insight into this complex issue and suggest some limits for future work. Even if the $^{207}Pb/^{206}Pb$ ages of the discordant grains were not to be discarded, it can be seen in fractions A to C (light-grey curves on Fig. 2) that the overall age distribution does not change significantly. It is in the two most-paramagnetic fractions, D and E, that significant problems emerge. Both fractions require the discarding of over 40% of the analyses—clearly inefficient use of analytical time. The age distributions also alter between the complete age data and concordant-only age data, with various modes altering markedly. Finally and more seriously, some of the supposedly concordant results show signs of unreliability. The age of the youngest mode in fractions D and E are ~10 Myr younger than the ~2960 Ma components seen in the other fractions. In addition, some "concordant" measurements in fraction E are below the minimum limiting age given by overlying volcaniclastics. This suggests that these apparently concordant grains have sufficient U content, metamictization, and related Pb-loss to cause slight discordance that is not detectable with this analytical method on an individual basis.

These results indicate that the most-paramagnetic fractions (D and E) are generally unreliable and their analysis is inefficient. A good compromise between representation and analytical efficiency/reliability occurs with fraction C at a Frantz separator setting of 1.8 A and 10° side-slope.

6.3. Provenance Interpretations

On a first pass, it could be stated that the least-paramagnetic fraction alone is sufficient to illustrate the age distribution because the major modes are present and their presence does not change in the other fractions. This view is challenged in two ways.

The results here indicate that this "sufficient" representation in the least-magnetic fraction cannot be assumed. The bulk of the ~2960 Ma ages occurs in Stage II metamictization between 3 and 8×10^{15} α-events/mg (Fig. 3). In this case, some of the ~2960 Ma mode have relatively lower U content and levels of metamictization and are seen in the least-paramagnetic fraction at the Frantz settings used for this study. Can this fortunate coincidence be automatically assumed to occur in all samples examined for detrital zircon geochronology? An even more rigourous setting, especially a diamagnetic setting (reverse slope on the Frantz chute), could easily eliminate the presence of this mode altogether. There are only five ~2960 Ma mode grains with α-doses below 2×10^{15} α-events/mg and none below 1×10^{15} α-events/mg.

The second argument against the apparently sufficient representation in the least-paramagnetic fraction involves the nature of the interpretation itself. While it has been acknowledged that quantitative provenance is not possible, this does not mean that the relative size of particular modes has no significance. For example, the prevalence of a particular mode occurring in multiple samples over a wide area would point to the importance of such rocks in the area being eroded. High throughput methods such as available with spot dating methods allow such statistical geochronology to be accomplished, and thus steps should be taken to avoid potential analytical biases, such as taking the least-magnetic fraction.

The study here illustrates what is possible with comparisons between the two principal age modes. By including data from fractions B and C, it can be seen that the ~2960 Ma age mode is more prevalent than would be considered using fraction A alone. This can be added to the provenance interpretation, because it indicates that the ~2960 Ma source was a major supplier of the sediment, possibly even more than the ~3150 Ma source. The concentration of the ~3150 Ma mode in the least-paramagnetic fraction suggests a compositional control and/or the selective destruction of ~3150 Ma grains with higher degrees of metamictization during transportation.

The latter interpretation is tempting, because it potentially offers further provenance information about distal and multicycle sources. However, as discussed below, further investigation of the results suggests the assumption of selective destruction during transportation needs careful consideration.

6.4. Metamictization, Sedimentary Transportation, and Paramagnetic Biasing

Grain survivability has been correlated in some cases with U content (Heaman and Parrish, 1991), but survivability depends on metamictization, which in turn depends on uranium content and, possibly most importantly, age. A high U grain will survive transportation through to deposition and subsequent analysis if transportation occurs before α-decay damage becomes too great. The combination of high-energy environments and relatively recent dominant sources (typically 650–150 Ma) can be seen in data from zircon in modern beach sand in eastern Australia (selected for SHRIMP analysis with Frantz settings at 2 A and 5° side-slope and non-biasing criteria; Sircombe, 1999). With over 800 analyses, the median α-dose is 0.44×10^{15} α-events/mg and the 95 percentile is 1.91×10^{15} α-events/mg. (The comparable U content values are 209 ppm and 629 ppm, respectively, again reinforcing the unsuitability of U content alone as a limit.) In comparison, for the Dwyer Lake metaquartzite, the 95 percentile of α-dose in fraction A alone is 5.7×10^{15} α-events/mg. By incorporating concordant results in fractions B and C, this rises to a 95 percentile at 8.5×10^{15} α-events/mg.

The comparison between the ancient Dwyer Lake sample and modern beach sand is relevant to the discussion of biasing here. As illustrated in Figure 4, metamictization is correlated to paramagnetism. Hence, this paramagnetic biasing may only occur when metamictization has reached a sufficient level. For instance, biasing is not a problem in the recent beach sands of eastern Australia, because metamictization has not occurred to the degree where the intrusion of Fe-compounds into the damaged lattice will induce paramagnetic biases during sample preparation.

Provenance interpretations explaining modes with restricted U content (such as the ~3150 Ma mode discussed above) by "loss of higher-U grains during transportation" are also incorrect if the time between formation and deposition is not accounted for. The 95 percentile of α-dose on modern beach sands at 1.91×10^{15} α-events/mg is taken as an indicator of the degree to which zircon metamictization is destroyed in a high-energy environment. Only those grains from the ~3150 Ma source with extreme U content of >1700 ppm would have reached such a level of α-dose in the ~300 Myr between formation and deposition. The time between formation and deposition in the ~2960 Ma mode is even shorter. The low U content and low α-dose in the ~3150 Ma mode (and conversely the relatively higher values in the ~2960 Ma mode) are taken as reflecting original source composition control rather than sedimentary processes.

6.5. Size, Magnetic Susceptibility, and Age

This set of data also provides an opportunity to assess the relation between zircon grain size in a sedimentary setting and such parameters as discordance and age. Partitioning of zircon samples based on size is often performed in conventional geochronology (Silver, 1963b; Silver and Deutsch, 1963). A correlation between size and age could also yield important provenance information.

However, in this sample, size is not correlated to either discordance (Fig. 5a) or concordant age (Fig. 5b). This suggests, at least for heterogeneous sedimentary zircon suites, that size is not related to discordance and is thus not a useful way to fractionate and select the "best" zircon samples. This example also indicates that zircon grain size may not be a diagnostic provenance feature in mature, well-sorted sediments.

7. CONCLUSIONS

Detrital zircon geochronology is subject to limitations imposed by natural and artificial biases. Natural biases are induced during sedimentary processes and are an acknowledged fact of any provenance analysis project. In contrast, artificial biases are induced during sample selection and preparation and can be monitored and mitigated. This study has focused on one of these artificial biases caused by paramagnetic fractionation during sample preparation using the Frantz magnetic barrier separator.

The results presented here further illustrate the known relationship between paramagnetism and U content/metamictization (Fig. 4). The data clearly illustrate that there is a bias in the distribution of ages depending on paramagnetism. The assumption that despite this biasing, the least-paramagnetic fraction remains sufficient for "there or not" interpretations is considered unreliable and, potentially, an unnecessary source of bias. The nature of the "there or not" provenance interpretation is also considered simplistic, and while a pure quantitative interpretation is not possible, further provenance information is available in a sample selected from a broader paramagnetic range.

The data presented also provide insight into other issues regarding detrital zircon geochronology and provenance interpretations. Careful consideration must be given to metamictization. Previous assumptions about U content and grain survival in sedimentary processes are too simplistic. In addition, paramagnetic biasing may only be an issue in Archean zircons in which sufficient metamictization has occurred to induce a range of paramagnetism. It is possible to differentiate in provenance interpretations between compositional control and possible losses during sedimentary transport by accounting for α-damage and the time between formation and deposition. A secondary issue is grain size, and at least for the heterogeneous sedimentary zircon suite from a mature sediment presented here, grain size has no control over grain discordance.

The management of discordant grains is always of concern in detrital zircon geochronology. While at the very least, including zircon grains from a broader paramagnetic range can only enhance

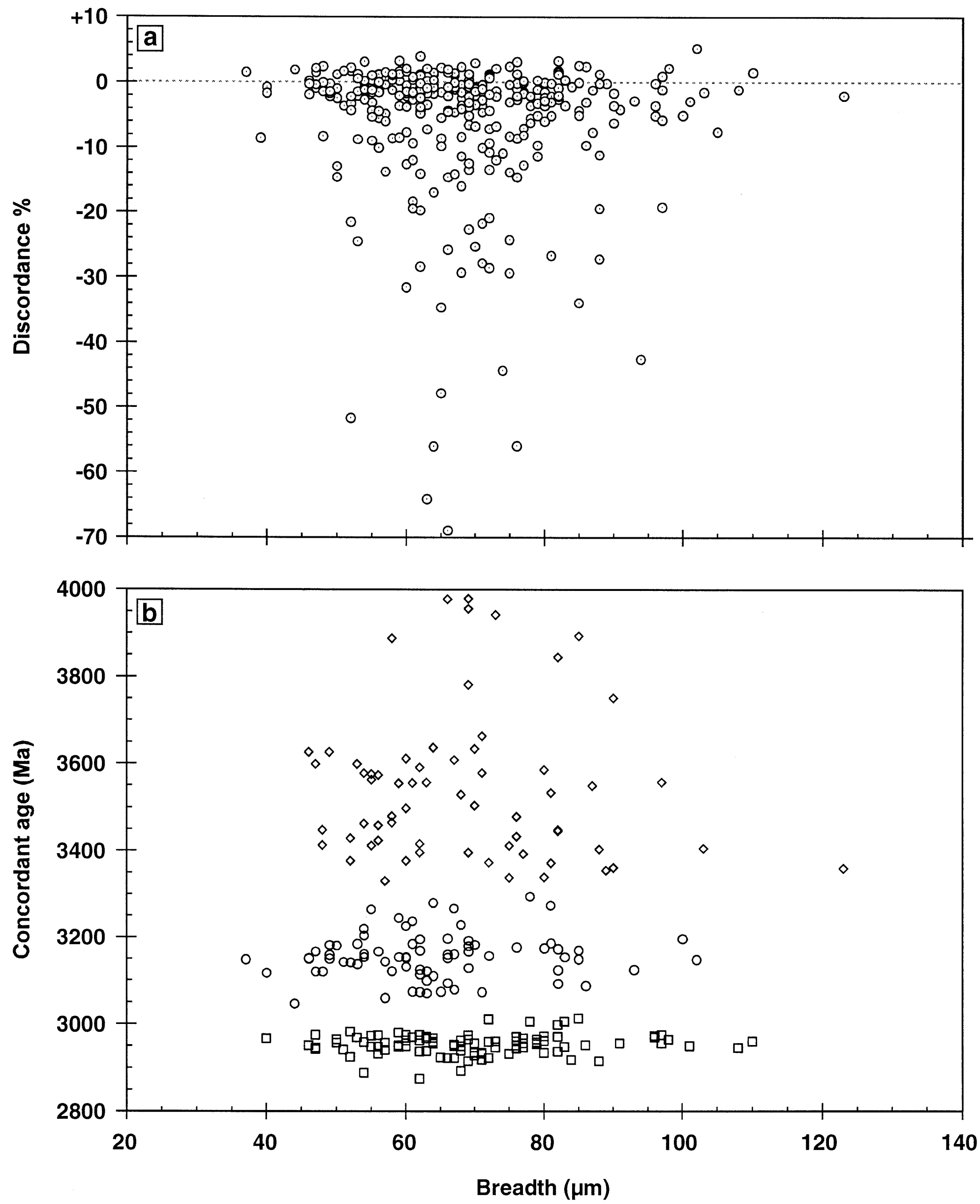

Fig. 5. Scatterplot illustrating the lack of relationship between (a) breadth and the discordance of all the analysed grains and (b) breadth and concordant $^{207}Pb/^{206}Pb$ ages only. Squares, circles, and triangles highlight the ages in the ~2960 Ma, ~3150 Ma, and >3300 Ma age components, respectively.

provenance interpretations, results from higher paramagnetic fractions become increasingly unreliable and thus analytically inefficient. The results of this study indicate that taking the nonmagnetic fraction of a detrital zircon sample at a Frantz setting of 1.8 A 10° side-slope, or a mass magnetic susceptibility of 4.72×10^{-7} e.m.u./g (5.93×10^{-9} m^3/kg), is a reasonable compromise between representation and analytical efficiency.

Acknowledgments—This paper greatly benefited from reviews by K. Ansdell, W. Bleeker, D. Davis, R. Ernst, V. McNicoll, and A. Nemchin. J. Sun (S.G. Frantz Co. Inc.) is thanked for his prompt and informative responses to inquiries. KNS acknowledges support of a NSERC Canadian Laboratories Visiting Fellowship. GSC Contribution number 2000196.

Associate editor: Y. Amelin

REFERENCES

Bleeker W. and Davis W. J. (1999) The 1991–1996 NATMAP Slave Province Project: Introduction. *Can. J. Earth Sci.* **36,** 1033–1042.

Bleeker W., Ketchum J. W. F., Jackson V. A., and Villeneuve M. E. (1999) The Central Slave Basement Complex; Part I, Its structural topology and autochthonous cover. *Can. J. Earth Sci.* **36,** 1083–1109.

Boggs S. J. (1995) *Principles of Sedimentology and Stratigraphy.* Merrill Publishing Company, 774 pp.

Davis D. W., Hirdes W., Schaltegger U., and Nunoo E. A. (1994) U-Pb age constraints on deposition and provenance of Birmian and gold-

bearing Tarkwaian sediments in Ghana, West Africa. *Precambrian Res.* **67,** 89–107.
Deer W. A., Howie R. A., and Zussman J. (1992) *An Introduction to the Rock Forming Minerals*. Longman Scientific and Technical, 696 pp.
Dodson M. H., Compston W., Williams I. S., and Wilson J. F. (1988) A search for ancient detrital zircons in Zimbabwean sediments. *J. Geol. Soc. London* **145,** 977–983.
Flinter B. (1959) The magnetic separation of some alluvial minerals in Malaya. *Am. Mineral.* **44,** 738–751.
Folk R. L. (1980) *Petrology of Sedimentary Rocks*. Hemphill Publishing Company, 182 pp.
Folk R. L. and Ward W. C. (1957) Brazos River bar; a study of the significance of grain size parameters. *J. Sediment. Petrol.* **27,** 3–26.
Gabenisch B., Zeller C., Camberlin V., and Bolfa J. (1972) Contribution a l'etude du separateur magnetique isodynamique de Frantz. *Bulletin Académie et Société Lorraines des Sciences* **11,** 2–53.
Gaudin A. and Spedden H. (1943) Magnetic separation of sulphide minerals. *American Institute of Mining and Metallurgical Engineers Transactions* **153,** 563–575.
Heaman L. and Parrish R. (1991) U-Pb geochronology of accessory minerals. In *Applications of Radiogenic Isotope Systems to Problems in Geology*, Vol. 19 (eds. L. Heaman and J. Ludden), 59–102. Mineralogical Association of Canada.
Isachsen C. E. and Bowring S. A. (1997) The Bell Lake Group and Anton Complex; A basement-cover sequence beneath the Archean Yellowknife greenstone belt revealed and implicated in greenstone belt formation. *Can. J. Earth Sci.* **34,** 169–189.
Kaye G. and Laby T. (1973) *Tables of Physical and Chemical Constants*. Longman, 386 pp.
Ketchum J. and Bleeker W. (2000) New field and U-Pb data from the Central Slave Cover Group near Yellowknife and the Central Slave Basement Complex at Point Lake. In *Slave-Northern Cordillera Lithospheric Evolution (SNORCLE) Transect and Cordilleran Tectonics Workshop Meeting*, Lithoprobe Report No. 72 (eds. F Cook and P Erdmer), 27–31. University of Calgary, 257 pp.
Krogh T. E. (1982) Improved accuracy of U-Pb zircon dating by selection of more concordant fractions using a high gradient magnetic separation technique. *Geochim. Cosmochim. Acta* **46,** 631–635.
Lewis R. and Senftle F. (1966) The source of ferromagnetism in zircon. *Am. Mineral.* **51,** 1467–1475.
McAndrew J. (1957) Calibration of a Frantz isodynamic separator and its application to mineral separation. *Proceedings of the Australasian Institute of Mining and Metallurgy* **181,** 59–73.
Morton A., Clauoe-Long J. C., and Berge C. (1996) SHRIMP constraints on sediment provenance and transport history in the Mesozoic Statfjord Formation, North Sea. *J. Geol. Soc. London* **153,** 915–929.
Murakami T., Chakoumakos B. C., Ewing R. C., Lumpkin G. R., and Weber W. J. (1991) Alpha-decay event damage in zircon. *Am. Mineral.* **76,** 1510–1532.
Oberteuffer J. A. (1974) Magnetic separation: A review of principles, devices and applications. *IEEE T. Magn.* **10,** 223–238.
Payne M. (1981) SI and Gaussian CGS units, conversions and equations for use in geomagnetism. *Phys. Earth Planet. In.* **26,** 10–16.
Powell H. and Ballard L.(1968) *Magnetic Susceptibility of Group IVb, Vb and VIb Metal-Bearing Minerals*, U.S. Department of the Interior, Bureau of Mines, Information Circular 8360, 9 p.
Rainbird R. H., Stern R. A., Khudoley A. K., Kropachev A. P., Heaman L. M., and Sukhorukov V. I. (1998) U-Pb geochronology of Riphean sandstone and agbbro from south-east Siberia and its bearing on the Laurentia-Siberia connection. *Earth Planet. Sci. Lett.* **164,** 409–420.
Rojas H., Cortelezzi C. R., and Ronco J. J. (1965) Separacion electromagnetica de minerales de arenas titaniferas de la zona de San Blas. *Acta Geol. Lilloana* **6,** 217–226.
Rosenblum S. (1958) Magnetic susceptibilities of minerals in the Frantz Isodynamic Magnetic Separator. *Am. Mineral.* **43,** 170–173.
Russ J. C. (1994) *The Image Processing Handbook*. CRC Press, 674 pp.
Sambridge M. S. and Compston W. (1994) Mixture modelling of multi-component data sets with application to ion-probe zircon ages. *Earth Planet. Sci. Lett.* **128,** 373–390.
Silver L. (1963a) The relation between radioactivity and discordance in zircons. *National Academy of Sciences—National Research Council Publication* **1075,** 34–52.
Silver L. (1963b) The use of cogenetic uranium-lead isotope systems in zircons in geochronology. *Radioactive Dating, International Atomic Energy Agency Symposium*, 279–287.
Silver L. and Deutsch S. (1963) Uranium-lead isotopic variations in zircon: a case study. *J. Geol.* **71,** 721–758.
Sircombe K. N. (1999) Tracing provenance through the isotope ages of littoral and sedimentary detrital zircon, eastern Australia. *Sediment. Geol.* **124,** 47–67.
Sircombe K. N. (2000a) Quantitative comparison of large sets of geochronological data using multivariate analysis: A provenance study example from Australia. *Geochim. Cosmochim. Acta* **64,** 1593–1616.
Sircombe K. N. (2000b) The utility and limitations of binned frequency histograms and probability density distributions for displaying absolute age data. Radiogenic age and isotopic studies—Report 13. *Geological Survey of Canada—Current Research* no. 2000-F2, 11 pp.
Sircombe K. N., Bleeker W., and Stern R. A. (2001) Detrital zircon geochronology and grain-size analysis of a ~2800 Ma Mesoarchean proto-cratonic cover succession, Slave Province, Canada. *Earth Planet. Sci. Lett.* **189,** 207–220.
Stern R. A.(1997) The GSC sensitive high ion microprobe (SHRIMP): Analytical techniques of zircon U-Th-Pb age determinations and performance evaluation. *Geological Survey of Canada—Current Research*, pp. 1–31.
Voigt W. and Kinoshita S. (1907) Bestimmung absoluter Werte von Magnetisierungszahlen, insbesondere für Kristalle. *Ann. Phys.-Leipzig* **24,** 492–514.

APPENDIX

OPERATION AND CALIBRATION OF THE FRANTZ MAGNETIC BARRIER SEPARATOR

Operation

There have been a number of descriptions of the operation of the Frantz magnetic separators (Gaudin and Spedden, 1943; McAndrew, 1957; Rojas et al., 1965; Gabenisch et al., 1972; Oberteuffer, 1974). Some of these descriptions were based on the earlier L-1 "Isodynamic" model and are often focused on a largely empirical approach to mineral separation (e.g., Rosenblum, 1958; Flinter, 1959). However, the theoretical basis for operation is largely the same for the LB-1 "Barrier" model. (The LB-1 model introduced pole pieces that produced a planar isodynamic magnetic field with an energy gradient approximately four times greater than the broad isodynamic field of the L-1—hence, the "magnetic barrier" nomenclature. This makes the LB-1 more sensitive in separating materials with low ranges of paramagnetic or diamagnetic susceptibilities. The sense of tilt on the side-slope is also reversed with paramagnetic materials being attracted toward the inner edge of the chute in the LB-1 rather than the outer edge of the L-1 chute as described in the earlier literature.)

The two principal forces that act on a grain moving down the chute are illustrated in Figure A1. The gravitational force, F_g, acts down the direction of maximum slope, while the magnetic force, F_m, inducted in the grain, acts perpendicularly to the chute. Following the nomenclature of McAndrew (1957) in CGS units:

$$F_m = \chi_g m H \frac{dH}{dx} \tag{1}$$

where a paramagnetic or diamagnetic particle has mass m grams and mass magnetic susceptibility χ_g and is acted on by a magnetic field with strength H oersteds (or gauss, assuming a free-space permeability of 1) and a gradient of dH/dx measured in distance of cm. The gravitational component acting across the chute is given by:

$$F'_g = mg \sin \theta \tag{2}$$

where g is the gravitational constant (980 cm/s^2) and θ is the side-slope of the chute (Fig. A1). The forward slope of the chute is not considered critical to the separation process, provided the rate of flow is slow

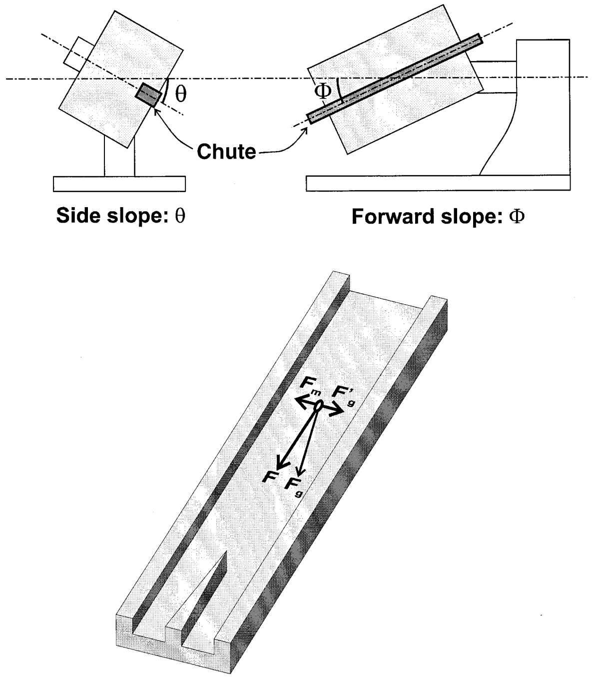

Fig. A1. Schematic illustration of the Frantz mechanical parameters and forces acting on a grain moving in the chute.

enough to allow grains moving in the chute to interact effectively with the magnetic barrier (McAndrew, 1957; Flinter, 1959). A forward slope of 10° was maintained throughout the separations described here.

Eqn. 1 and 2 can be combined to provide a calculation of mass magnetic susceptibility:

$$\chi_g = g \sin \theta \frac{1}{H} \frac{dx}{dH} \text{ (emu/g)} \tag{3}$$

This can be converted to SI values by multiplying by $4\pi/1000$. The value of magnetic energy gradient for a given setting of the electromagnet current can be determined using two methods described below.

Magnetic Energy Gradient: Theoretical Calculation

The strength of the magnetic energy gradient (*HdH/dx*) at the magnetic barrier of the LB-1 is illustrated in Figure A2 using data supplied by S. G. Frantz Co. Ltd. Using a modified sigmoid function, this relationship can be modeled as:

$$H\frac{dH}{dx} = \left(\frac{0.0038544}{0.00032445 + e^{-10.296i}} + \frac{1.0511}{0.037619 + e^{-3.051i}} - 1.0168\right) \times 10^7 \tag{4}$$

where i is the electromagnetic current in amperes. This calculation of magnetic energy gradient can then be used in Eqn. 3 to calculate magnetic susceptibility at various side-slope angle settings as illustrated in Figure A3. However, it must be acknowledged that these values are theoretical only. The actual strength of the magnetic field produced by any individual Frantz separator depends on the state of the electromagnet and the accuracy of the current meter. These features will undoubtedly vary from machine to machine, but the significance and range of the resulting inconsistency is unknown at this stage. Ideally, paramagnetic fractions should be reported in absolute terms of mass magnetic susceptibility that is then independent of any individual Frantz machine. As a step toward this, a method for direct calibration of an individual Frantz machine is described below.

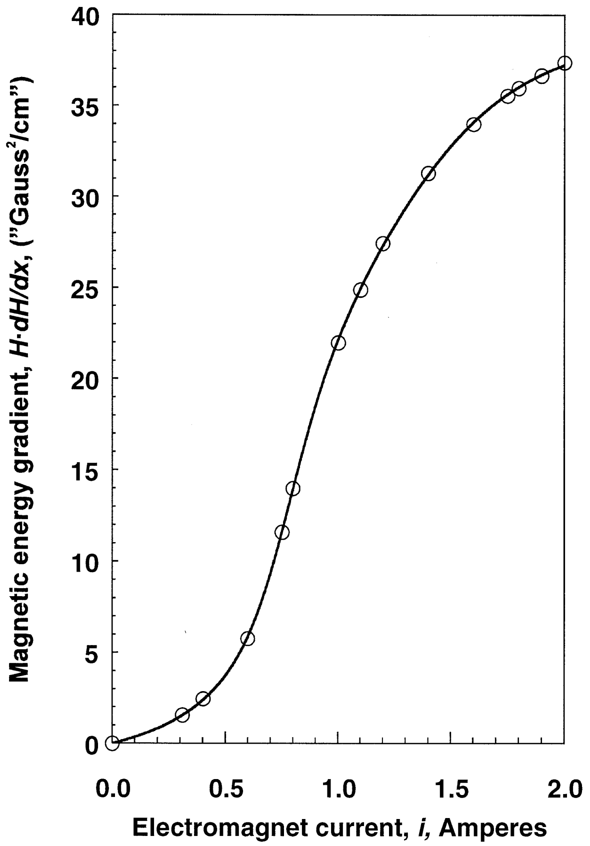

Fig. A2. Graph illustrating the magnetic energy gradient vs. electromagnet current for the LB-1 magnetic barrier separator. Based on graph supplied by S.G. Frantz Co. Inc.

Magnetic Energy Gradient: Direct Calibration

McAndrew (1957) presented a method for calibrating the L-1 separator, and although the calculations do not directly apply to the LB-1 separator, the methodology can be applied. By equating Eqn. 1 and 2:

$$\frac{\sin \theta}{\chi_g} = \frac{1}{g} H \frac{dH}{dx} \tag{5}$$

and assuming that the magnetic field strength will increase at the same rate as the electromagnet current, particularly at low currents, Eqn. 4 can be written as a power-law relationship:

$$\frac{\sin \theta}{\chi_g} = ki^n \tag{6}$$

where i is the electromagnet current, n is a constant close to 2, and k has a constant value. Applying this relationship, McAndrew (1957) used substances of known magnetic susceptibility to find the calibration for the L-1 separator ($n = 2$, $k = 52{,}000$). Using data from S.G. Frantz that directly defines the relationship between magnetic field strength and electromagnet current for the L-1 separator, the derived calibration is close to that based on direct measurement of the magnetic field for electromagnet current values from ~0.5 to 1.0 A. A similar approach was used to check the calibration of the LB-1 separator used in this study.

Two inorganic compounds used by McAndrew (1957), ammonium iron(II) sulphate, $Fe(NH_4)_2(SO_4)_2 0.6H_2O$, and copper (II) sulphate, $CuSO_4 0.5H_2O$, were selected as having mass magnetic susceptibilities suitable for calibrating the Frantz separator at 32.3×10^{-6} e.m.u./g (40.6×10^{-8} m³/kg) and 6.13×10^{-6} e.m.u./g (7.7×10^{-8} m³/kg), respectively, at 20°C (Kaye and Laby, 1973). One limitation is that these substances tend to be only practically useful in the lower range of

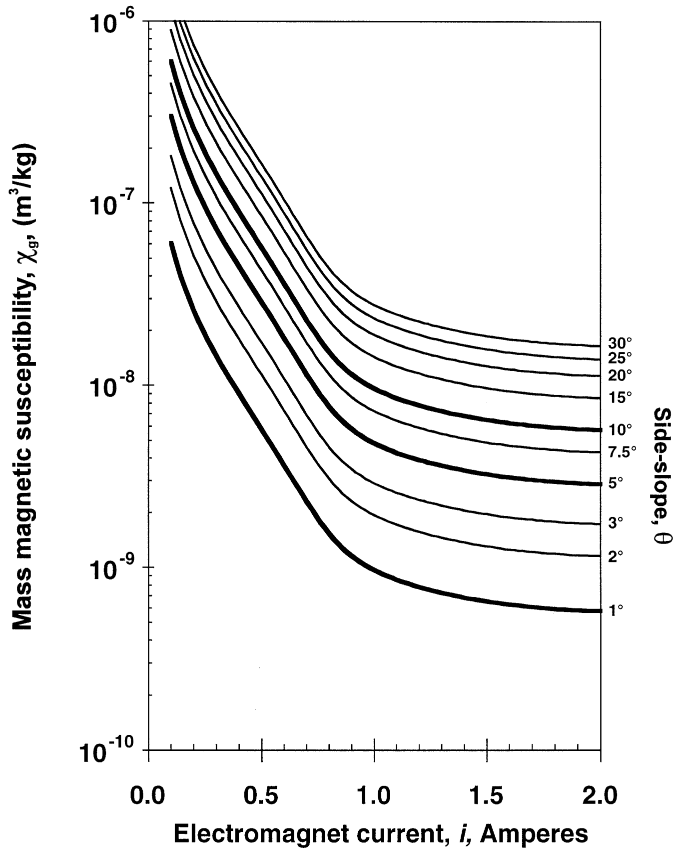

Fig. A3. Graph illustrating the relation between Frantz settings (side-slope and electromagnet current) and magnetic susceptibility derived using calculations for the magnetic energy gradient as discussed in the Appendix.

electromagnet current/magnetic field strength, thus requiring extrapolation of the results to higher field strengths more typical of zircon separation.

The separation process used during calibration was identical to that typically used in mineral separations. Materials used were sieved at 48 mesh (~340 microns) to remove large crystals. Material moved from the inside chute toward the magnetic barrier under the influence of gravity, depending on the side-slope. The electromagnet current was increased until a balance between the amount of material flowing along and passing through the barrier was achieved. These measurements are shown in Table A1 and plotted in Figure A4. The resulting best fit ($R = 0.99$) power-law equation results in $k = 87686$ and $n = 1.0821$.

Figure A5 illustrates a comparison between the two methods for calculating magnetic susceptibility as discussed above. The two calculations are within an order of magnitude of each other, indicating that the Frantz separator used in this study is not a radical departure from the expected magnetic field strength. However, it does highlight that the assumption of a power-law relationship between current and magnetic energy gradient is too simplistic for the LB-1 separator. Further work is required, particularly with substances with lower magnetic susceptibility that is closer to that commonly seen in zircon, to fully develop the Frantz calibration method into an independent test of magnetic field behavior. In the interim, the magnetic susceptibility values discussed in this study have been calculated using Eqn. 3 and 4.

Supplementary data tables

GSC Sample ID: BNB97-008
GSC Geochronology ID: Z6238
GSC Ion-probe mount ID: IP125
Topographic map location: 85-J 9637275E 6953175N
Latitude/Longitude: 62°41'6.8″N 114°19'5.6″W

Uncertainties reported at one sigma and are calculated by numerical
Uncertainties reported at one sigma and are calculated by numerical
propagation of all known sources of error (Stern, 1997). Data have been corrected for common-Pb according to procedures outlined in Stern (1997).

Spot name: Unique identification of spot analysis, in the form

Table A1 Frantz separator electromagnet amperage settings required to paramagnetically balance streams of ammonium iron(II) sulphate and copper (II) sulphate in the chute at various side-slopes.

Side-slope	2.5	5.5	8	10.5	13	15.5	18	20.5	25.5	30.5
Substance					*Electromagnet amps*					
$Fe(NH_4)2(SO_4)_2.6H_2O$			0.05	0.075	0.10	0.12	0.14	0.15	0.175	0.225
$CuSO_4.5H_2O$	0.10	0.25		0.35		0.55		0.60	0.70	

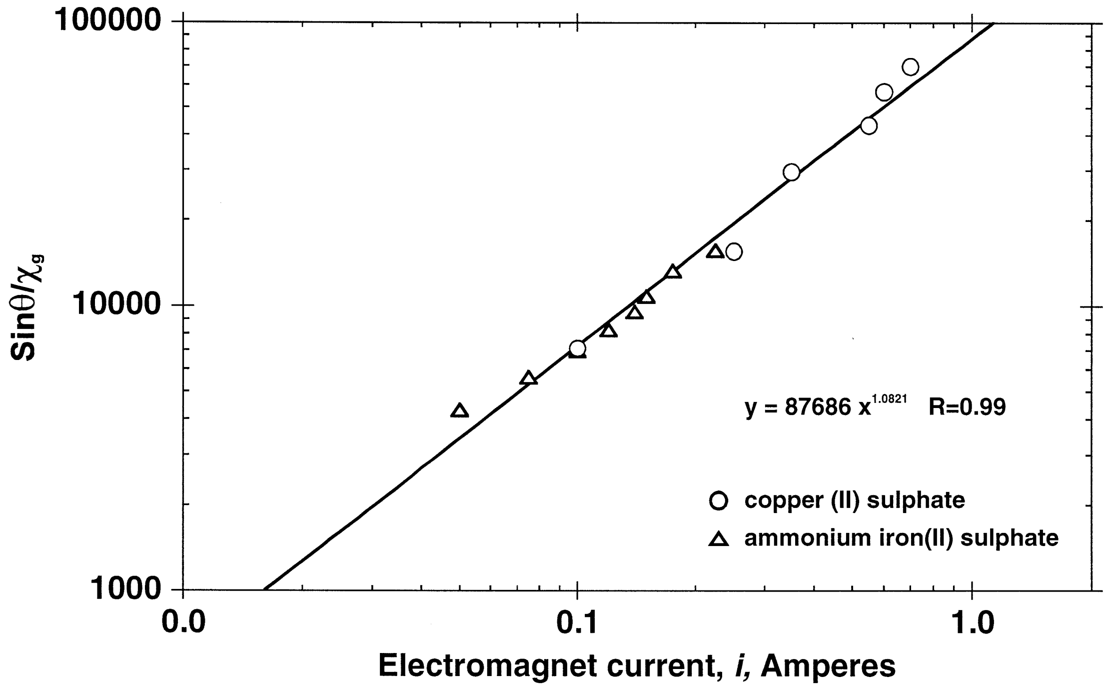

Fig. A4. Graph illustrating the direct calibration measurements using substances of known magnetic susceptibility on the Frantz magnetic barrier separator.

grain-number · spot-number, e.g. 12.2 is the 2nd spot on grain 12. 'C' indicates an analysis on a suspected core area of a grain, 'R' indicates an analysis on a suspected rim. † indicates spots < 95% concordant, ‡ indicates spots >105% concordant, § indicates spots that have been discarded from further interpretation because of extreme error related to analytical problems, high common-Pb content or are erroneously younger than geochronologic constraints in the case of Fraction E as discussed in text.

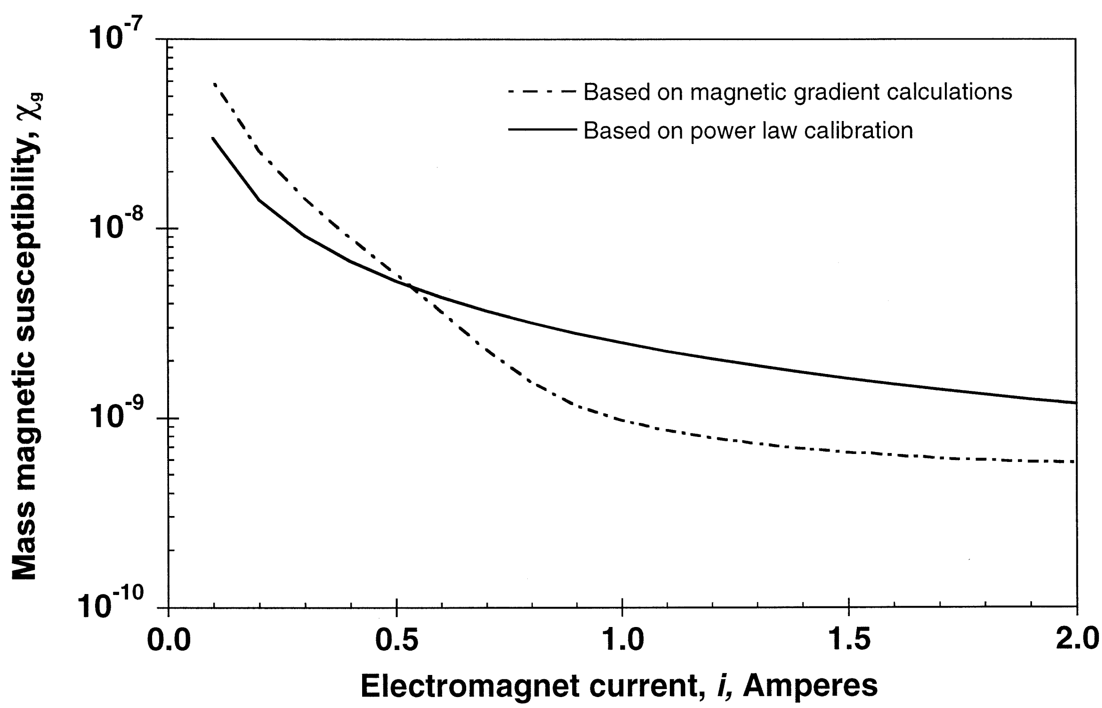

Fig. A5. Graph illustrating the comparison between magnetic susceptibility values derived by using a calculation of magnetic energy gradient and values derived from a power-law relation based on direct measurement of substances of known magnetic susceptibility.

U (ppm): Parts per million uranium abundance. Calculated by calibration against Zr20 in standard zircon.

Th (ppm): Parts per million thorium abundance. Calculated by calibration with U content.

Th/U: Thorium to uranium abundance ratio.

Pb (ppm): Parts per million radiogenic Pb content.

204Pb (ppb): Parts per billion 204(common) Pb content.

204Pb/206Pb: As directly measured.

f206: Refers to mole fraction of total 206Pb that is due to common Pb. Calculated with 204Pb method. A negative value indicates where common Pb content is calculated as less than background.

208Pb/206Pb: As directly measured.

206Pb/238U: As calculated by calibration to standard zircon.

207Pb/206Pb: As directly measured.

Apparent Ages (Ma): Apparent age calculated from 204Pb-corrected 206Pb*/238U and 207Pb/206Pb ratios.

Conc.%: 100 $\times$ (206Pb/238U age)/(207Pb/206Pb age).

Disc. %: 100 $-$ concordance%

Alpha-dose: alpha-dose as calculated using formula in Murakami et al. (1991)

Breadth: Minimum axis of digitized image in μm.

Length: Maximum axis of digitized image in μm.

EqDiam: Equivalent diameter of a circle encompassing the same area as the grain.

Form factor: An estimate of roundness varying from 0 to 1 for a perfect circle, defined by $4\pi \cdot$ area/perimeter^2; (Russ, 1994, p. 525).

Dwyer Lake Quartzite, Slave Province, Magnetic Fraction A 1.8A 1°NM

Spot name	U (ppm)	Th (ppm)	Th/U	Pb (ppm)	204Pb (ppb)	204Pb/206Pb	±204Pb/206Pb	f206	208Pb/206Pb	±208Pb/206Pb	206Pb/238U	±206Pb/238U	207Pb/235U	±207Pb/235U	207Pb/206Pb	±207Pb/206Pb	Apparent Ages (Ma) 206Pb/238U	±206Pb/238U	207Pb/206Pb	±207Pb/206Pb	Conc.%	Disc.%	a-dose events/mg x 10^15	Breadth µm	Length µm	EqDiam µm	Form Factor
A-39.1	129	74	0.59	90	55	0.00083	0.00014	0.01092	0.16815	0.01163	0.58734	0.01419	17.218	1.900	0.21261	0.02225	2978.7	57.9	2925.5	180.3	101.8	-1.8	1.94	52	118	76	0.67
A-58.1	135	90	0.68	93	15	0.00022	0.00007	0.00291	0.18169	0.01025	0.57480	0.02572	16.916	1.138	0.21344	0.00960	2927.5	106.2	2931.9	74.6	99.9	0.1	2.08	56	93	71	0.80
A-27.1	199	86	0.45	133	48	0.00048	0.00237	0.00631	0.11388	0.07824	0.58654	0.02822	17.316	3.122	0.21411	0.03594	2975.4	115.7	2936.9	301.0	101.3	-1.3	2.94	62	97	75	0.79
A-15.1	199	141	0.73	139	125	0.00125	0.00019	0.01645	0.19363	0.03045	0.57494	0.07373	16.987	3.378	0.21429	0.02931	2928.1	309.1	2938.3	240.2	99.7	0.3	3.09	63	74	67	0.75
A-16.1	292	142	0.50	201	22	0.00015	0.00014	0.00193	0.13606	0.00959	0.59268	0.02666	17.561	1.370	0.21490	0.01254	3000.3	108.8	2942.9	97.6	102.0	-2.0	4.37	47	85	62	0.70
A-37.1	213	107	0.52	143	23	0.00022	0.00009	0.00292	0.14174	0.01013	0.57359	0.02807	17.017	1.233	0.21517	0.01026	2922.6	116.1	2944.9	79.2	99.2	0.8	3.21	76	100	85	0.80
A-55.1	133	79	0.61	93	14	0.00021	0.00016	0.00270	0.15342	0.00638	0.58952	0.02576	17.525	0.822	0.21561	0.00267	2987.5	105.3	2948.2	20.2	101.3	-1.3	2.04	56	76	62	0.82
A-56.1	379	180	0.49	255	5	0.00002	0.00008	0.00032	0.12898	0.00457	0.58247	0.01056	17.353	1.781	0.21607	0.02135	2958.8	43.2	2951.6	169.2	100.2	-0.2	5.69	46	79	54	0.60
A-60.1	353	109	0.32	217	30	0.00018	0.00042	0.00234	0.07808	0.01411	0.55229	0.06038	16.503	2.092	0.21672	0.01126	2834.7	255.8	2956.5	86.5	95.9	4.1	5.17	91	100	94	0.79
A-8.1	427	232	0.56	298	18	0.00008	0.00002	0.00110	0.14978	0.00869	0.59381	0.01431	17.780	0.551	0.21716	0.00363	3004.9	58.1	2959.8	27.2	101.5	-1.5	6.51	64	130	93	0.69
A-4.1	267	173	0.67	183	11	0.00008	0.00012	0.00110	0.17636	0.01258	0.57068	0.01191	17.124	3.230	0.21762	0.04024	2910.6	49.1	2963.2	334.6	98.2	1.8	4.15	60	83	68	0.79
A-48.1	276	183	0.68	193	17	0.00012	0.00010	0.00163	0.18014	0.01513	0.58186	0.01347	17.512	1.020	0.21828	0.01105	2956.4	55.1	2968.1	84.0	99.6	0.4	4.31	64	84	70	0.83
A-42.1	377	146	0.40	251	12	0.00006	0.00004	0.00082	0.11022	0.00176	0.58069	0.01233	17.553	0.402	0.21923	0.00139	2951.6	50.5	2975.1	10.2	99.2	0.8	5.66	47	80	59	0.71
A-32.1	53	16	0.31	37	48	0.00166	0.00030	0.02130	0.06559	0.03912	0.61842	0.09181	19.544	4.549	0.22921	0.03706	3103.6	376.5	3046.5	285.9	101.9	-1.9	0.82	44	73	57	0.74
A-19.1	77	17	0.23	53	13	0.00032	0.00148	0.00410	0.05598	0.04826	0.62653	0.02001	20.100	2.561	0.23267	0.02778	3135.9	79.8	3070.5	205.0	102.1	-2.1	1.18	63	88	70	0.59
A-25.1	60	45	0.77	48	14	0.00042	0.00011	0.00539	0.21199	0.03532	0.64221	0.22251	20.640	7.578	0.23309	0.01996	3197.7	938.6	3073.4	143.9	104.0	-4.0	0.99	62	91	73	0.80
A-1.1	94	2	0.02	61	0	0.00001	0.00211	0.00013	0.02734	0.06862	0.59162	0.02875	19.032	2.869	0.23332	0.03190	2996.0	117.5	3074.9	237.3	97.4	2.6	1.40	61	168	99	0.57
A-12.1	51	24	0.48	38	6	0.00023	0.00015	0.00292	0.12121	0.02359	0.62883	0.11450	20.230	4.553	0.23332	0.02600	3145.0	469.9	3075.0	190.3	102.3	-2.3	0.82	65	113	83	0.55
A-61.1	89	29	0.34	63	18	0.00038	0.00064	0.00484	0.08634	0.02562	0.62294	0.03803	20.093	2.100	0.23393	0.01813	3121.6	152.9	3079.2	129.5	101.4	-1.4	1.39	67	97	74	0.75
A-22.1	31	19	0.65	24	3	0.00016	0.00059	0.00199	0.15595	0.01965	0.63368	0.06561	20.555	2.364	0.23525	0.00912	3164.1	264.3	3088.2	63.3	102.5	-2.5	0.51	86	136	110	0.78
A-20.1†	326	196	0.62	207	477	0.00311	0.00023	0.04062	0.18577	0.01328	0.52574	0.06752	15.814	2.648	0.21815	0.02020	2723.5	291.8	2967.1	157.7	91.8	8.2	5.04	48	95	66	0.64
A-21.1†	61	20	0.34	41	20	0.00065	0.00031	0.00812	0.08807	0.02362	0.59007	0.01514	20.231	0.827	0.24867	0.00716	2989.7	61.7	3176.3	46.4	94.1	5.9	1.00	57	74	61	0.68
A-65.1	75	44	0.61	56	48	0.00119	0.00223	0.01512	0.16007	0.07554	0.61863	0.04825	20.211	3.719	0.23695	0.03725	3104.5	195.1	3099.6	275.9	100.2	-0.2	1.24	63	153	98	0.36
A-62.1	65	11	0.18	44	26	0.00075	0.00100	0.00956	0.03976	0.03373	0.60913	0.03732	20.120	1.881	0.23956	0.01518	3066.5	151.3	3117.1	104.7	98.4	1.6	1.01	40	75	55	0.70
A-30.1	126	20	0.16	89	8	0.00012	0.00029	0.00148	0.04661	0.01339	0.64231	0.10087	21.257	5.018	0.24003	0.03785	3198.1	408.6	3120.1	276.3	102.5	-2.5	1.95	48	71	55	0.77
A-5.1	34	25	0.75	27	8	0.00046	0.00009	0.00578	0.20872	0.00490	0.63492	0.01083	21.015	0.760	0.24005	0.00716	3169.0	42.8	3120.3	48.3	101.6	-1.6	0.58	47	66	53	0.78
A-45.1	111	54	0.50	83	20	0.00033	0.00337	0.00421	0.14986	0.11385	0.62581	0.04577	20.724	5.013	0.24017	0.05322	3133.0	184.1	3121.1	405.6	100.4	-0.4	1.83	58	132	82	0.47
A-54.2	237	73	0.32	165	18	0.00014	0.00043	0.00184	0.08917	0.01406	0.61018	0.01576	20.209	0.864	0.24020	0.00745	3070.7	63.4	3121.3	50.3	98.4	1.6	3.78	63	109	84	0.74
A-59.1	218	144	0.68	167	919	0.00708	0.00224	0.09002	0.16256	0.07723	0.63222	0.02794	20.992	3.331	0.24082	0.03539	3158.4	111.3	3125.4	255.6	101.1	-1.1	3.68	62	69	64	0.81
A-7.1	48	31	0.66	36	6	0.00025	0.00034	0.00318	0.17701	0.05057	0.62526	0.04876	20.799	2.441	0.24126	0.01895	3130.8	196.3	3128.3	130.8	100.1	-0.1	0.80	69	140	93	0.62
A-50.1	150	109	0.75	119	27	0.00033	0.00019	0.00418	0.20918	0.00812	0.63737	0.01047	21.330	0.589	0.24271	0.00491	3178.7	41.4	3137.9	32.5	101.3	-1.3	2.57	53	96	69	0.74
A-29.1	80	42	0.55	61	29	0.00064	0.00174	0.00813	0.13622	0.05707	0.64632	0.01984	21.678	2.464	0.24326	0.02570	3213.8	78.1	3141.5	178.7	102.3	-2.3	1.33	52	101	71	0.72
A-38.1	105	51	0.50	81	20	0.00034	0.00008	0.00436	0.14300	0.02550	0.64225	0.10543	21.557	5.358	0.24343	0.04070	3197.9	427.8	3142.5	294.3	101.8	-1.8	1.75	51	69	58	0.75
A-24.1	60	50	0.87	49	16	0.00048	0.00066	0.00611	0.22201	0.12502	0.64309	0.13724	21.677	6.887	0.24447	0.05138	3201.2	562.3	3149.3	380.7	101.6	-1.6	1.05	37	62	48	0.78
A-28.1	88	27	0.32	63	45	0.00093	0.00112	0.01174	0.07883	0.03835	0.62852	0.08211	21.200	4.259	0.24463	0.03355	3143.7	333.5	3150.4	236.5	99.8	0.2	1.43	46	58	51	0.85
A-36.1	45	16	0.37	32	2	0.00010	0.00006	0.00131	0.10137	0.01441	0.61335	0.06362	20.703	3.151	0.24481	0.02428	3083.4	259.4	3151.5	166.9	97.8	2.2	0.73	49	95	66	0.67
A-18.1	150	83	0.57	113	18	0.00022	0.00012	0.00282	0.16799	0.00730	0.61656	0.02117	20.814	1.091	0.24484	0.00870	3096.2	85.0	3151.7	57.6	98.2	1.8	2.53	46	76	57	0.73
A-9.1	57	31	0.56	42	2	0.00006	0.00006	0.00072	0.14968	0.00729	0.62067	0.02398	20.965	1.386	0.24498	0.01202	3112.6	96.1	3152.6	80.1	98.7	1.3	0.95	60	75	64	0.74
A-11.1	105	93	0.91	83	2	0.00004	0.00049	0.00053	0.25407	0.02158	0.61538	0.07768	20.799	2.810	0.24513	0.00857	3091.5	317.7	3153.6	56.6	98.0	2.0	1.86	59	82	69	0.76
A-33.1	119	56	0.49	89	18	0.00027	0.00331	0.00343	0.13233	0.10747	0.62964	0.04207	21.283	4.651	0.24516	0.04900	3148.2	168.6	3153.8	359.3	99.8	0.2	1.98	54	84	63	0.73
A-34.1	77	64	0.86	62	16	0.00038	0.00022	0.00475	0.23938	0.00731	0.63427	0.01192	21.445	1.096	0.24522	0.01110	3166.5	47.2	3154.1	73.7	100.4	-0.4	1.35	83	156	110	0.57
A-17.1	51	27	0.54	39	4	0.00013	0.00075	0.00164	0.16364	0.02936	0.62715	0.05216	21.305	2.836	0.24638	0.02317	3138.3	210.0	3161.6	157.7	99.3	0.7	0.87	54	81	64	0.72
A-26.1	94	30	0.33	71	18	0.00034	0.00009	0.00422	0.08177	0.01772	0.65588	0.03819	22.397	1.921	0.24766	0.01389	3251.2	150.4	3169.9	91.8	102.6	-2.6	1.54	85	126	97	0.75
A-51.1	64	26	0.43	48	8	0.00022	0.00232	0.00276	0.13087	0.07514	0.63070	0.02391	21.685	3.173	0.24937	0.03408	3152.4	95.2	3180.7	235.0	99.1	0.9	1.07	50	104	71	0.72
A-64.1	68	30	0.45	51	18	0.00048	0.00056	0.00603	0.12259	0.02624	0.62775	0.08756	21.636	4.630	0.24997	0.03645	3140.7	356.4	3184.6	252.1	98.6	1.4	1.15	53	79	57	0.64
A-26.2	94	35	0.38	68	14	0.00029	0.00066	0.00358	0.09790	0.02154	0.62298	0.01257	21.633	0.996	0.25185	0.00980	3121.8	50.1	3196.4	63.0	97.7	2.3	1.57	*	*	*	*
A-44.1	140	62	0.46	107	19	0.00025	0.00004	0.00304	0.11223	0.01613	0.64644	0.06473	23.443	2.930	0.26301	0.01666	3214.3	258.6	3264.8	103.4	98.5	1.5	2.45	55	87	69	0.80
A-53.1	57	46	0.83	49	17	0.00052	0.00040	0.00644	0.24413	0.04133	0.65776	0.01765	24.086	0.960	0.26558	0.00698	3258.5	69.0	3280.1	41.9	99.3	0.7	1.07	64	87	71	0.68
A-49.1	68	1	0.01	52	26	0.00064	0.00077	0.00778	0.00286	0.02826	0.69051	0.01746	26.105	1.389	0.27419	0.01200	3384.6	66.9	3330.2	70.3	101.6	-1.6	1.15	57	113	80	0.76
A-3.1	225	81	0.37	183	16	0.00012	0.00017	0.00142	0.09601	0.01202	0.68628	0.02712	26.647	1.532	0.28160	0.01045	3368.4	104.5	3371.9	59.1	99.9	0.1	4.10	81	104	87	0.81
A-14.1	93	34	0.37	77	6	0.00011	0.00118	0.00130	0.09715	0.03794	0.69445	0.01701	27.332	2.052	0.28545	0.01941	3399.6	65.1	3393.0	110.1	100.2	-0.2	1.72	77	100	83	0.67
A-43.1	77	30	0.40	63	12	0.00027	0.00206	0.00324	0.10429	0.06584	0.68554	0.02340	27.335	3.048	0.28919	0.02949	3365.6	90.1	3413.3	168.4	98.6	1.4	1.43	48	96	66	0.70
A-41.1	107	77	0.75	95	12	0.00019	0.00324	0.00230	0.19111	0.10340	0.69788	0.03833	27.872	6.016	0.28966	0.05850	3412.6	147.2	3415.8	355.7	99.9	0.1	2.10	62	129	89	0.73
A-57.1	105	26	0.26	85	4	0.00007	0.00022	0.00083	0.06728	0.00768	0.68759	0.02575	27.593	1.508	0.29105	0.01031	3373.4	99.1	3423.2	56.2	98.5	1.5	1.93	56	94	70	0.31
A-6.1	89	80	0.94	84	2	0.00004	0.00010	0.00045	0.25482	0.02444	0.70718	0.01293	28.837	0.714	0.29574	0.00431	3447.8	49.0	3448.1	22.8	100.0	0.0	1.81	48	86	63	0.76
A-35.1	14	6	0.40	12	11	0.00138	0.00046	0.01639	0.12277	0.01807	0.67000	0.03437	27.505	2.076	0.29774	0.01469	3305.9	134.1	3458.5	78.7	95.6	4.4	0.27	56	66	58	0.82
A-52.1	158	101	0.66	141	64	0.00066	0.00043	0.00780	0.16232	0.01680	0.71316	0.06114	29.347	3.217	0.29845	0.01744	3470.4	234.3	3462.2	93.7	100.2	-0.2	3.13	54	88	67	0.78
A-2.1	83	17	0.22	69	303	0.00565	0.00058	0.06657	0.06499	0.02727	0.70231	0.03206	30.268	3.010	0.31257	0.02589	3429.4	122.6	3533.7	134.0	97.0	3.0	1.60	81	130	99	0.74
A-13.1	96	66	0.70	90	5	0.00009	0.00025	0.00105	0.18501	0.01232	0.72641	0.06173	31.908	2.942	0.31858	0.00852	3520.0	234.7	3563.0	41.8	98.8	1.2	2.02	55	103	75	0.74
A-46.1	207	38	0.19	188	44	0.00032	0.00008	0.00368	0.04390	0.00584	0.77324	0.07106	34.296	4.704	0.32169	0.02927	3692.5	263.6	3577.9	147.4	103.2	-3.2	4.07	54	110	69	0.60
A-40.1	55	22	0.41	51	2	0.00006	0.00089	0.00073	0.11292	0.02826	0.74464	0.04124	33.482	2.407	0.32611	0.01287	3587.7	154.2	3598.9	61.9	99.7	0.3	1.13	47	67	55	0.81
A-47.1	349	26	0.08	304	64	0.00028	0.00004	0.00328	0.01911	0.00148	0.75363	0.01933	33.890	1.624	0.32615	0.01220	3620.9	71.5	3599.1	58.6	100.6	-0.6	6.81	53	93	68	0.78
A-63.1	140	27	0.20	122	43	0.00048	0.01239	0.00558	0.04431	0.38958	0.74077	0.14535	33.898	20.138	0.33188	0.17814	3573.4	562.1	3625.8	1237.8	98.6	1.4	2.81	49	63	53	0.83
A-31.1	165	110	0.69	162	18	0.00017	0.00151	0.00195	0.18333	0.04773	0.75277	0.01956	34.455	3.067	0.33196	0.02721	3617.7	72.3	3626.2	131.6	99.8	0.2	3.57	46	75	58	0.80
A-23.1	363	222	0.63	412	177	0.00067	0.00009	0.00728	0.16847	0.01567	0.84259	0.07295	45.842	5.686	0.39459	0.03104	3939.9	260.4	3888.6	123.8	101.3	-1.3	8.86	58	128	86	0.69
A-10.2	66	31	0.50	73	12	0.00026	0.00018	0.00277	0.14036	0.00832	0.84061	0.03125	47.178	2.996	0.40704	0.01915	3933.0	110.4	3935.3	72.5	99.9	0.1	1.61	*	*	*	*
A-10.1	47	22	0.49	54	2	0.00007	0.00031	0.00077	0.13294	0.01684	0.86703	0.01600	48.858	1.137	0.40870	0.00493	4024.8	55.5	3941.4	18.2	102.1	-2.1	1.15	73	114	92	0.73

Dwyer Lake Quartzite, Slave Province, Magnetic Fraction 'B' 1.8A 1°M

Spot name	U (ppm)	Th (ppm)	Th/U	Pb (ppm)	204Pb (ppb)	204Pb/ 206Pb	±204Pb/ 206Pb	f206	208Pb/ 206Pb	±208Pb/ 206Pb	206Pb/ 238U	±206Pb/ 238U	207Pb/ 235U	±207Pb/ 235U	207Pb/ 206Pb	±207Pb/ 206Pb	Apparent Ages (Ma) 206Pb/ 238U	±206Pb/ 238U	207Pb/ 206Pb	±207Pb/ 206Pb	Conc.%	Disc.%	a-dose events/mg x 10^15	Breadth µm	Length µm	EqDiam µm	Form Factor
B-10.1	250	122	0.50	169	12	0.00009	0.00007	0.00122	0.13591	0.01026	0.58263	0.01457	17.046	0.599	0.21219	0.00461	2959.5	59.6	2922.3	35.6	101.3	-1.3	3.71	72	126	93	0.75
B-3.1	193	100	0.54	134	11	0.00011	0.00043	0.00142	0.13862	0.01428	0.59792	0.01047	17.620	0.646	0.21373	0.00643	3021.5	42.4	2934.0	49.5	103.0	-3.0	2.90	70	99	82	0.76
B-24.1	321	121	0.39	204	370	0.00234	0.00022	0.03072	0.11081	0.01809	0.55723	0.05088	16.422	2.607	0.21374	0.02542	2855.2	214.1	2934.1	206.6	97.3	2.7	4.70	71	149	100	0.61
B-59.1	278	123	0.46	184	38	0.00028	0.00116	0.00360	0.12386	0.04107	0.57405	0.03197	17.040	2.996	0.21528	0.03443	2924.4	132.3	2945.8	285.0	99.3	0.7	4.15	47	89	63	0.67
B-4.1	143	103	0.75	101	7	0.00010	0.00012	0.00137	0.20600	0.00822	0.57424	0.01047	17.086	0.394	0.21580	0.00260	2925.2	43.0	2949.6	19.6	99.2	0.8	2.23	67	104	79	0.73
B-47.1†	169	70	0.43	101	53	0.00070	0.00012	0.00914	0.12671	0.03283	0.51974	0.03485	15.482	1.856	0.21604	0.01973	2698.1	149.5	2951.4	155.7	91.4	8.6	2.51	58	83	64	0.71
B-17.1	228	140	0.63	157	12	0.00010	0.00002	0.00134	0.17033	0.00858	0.57403	0.02249	17.151	1.353	0.21669	0.01381	2924.4	92.8	2956.3	106.8	98.9	1.1	3.52	97	119	99	0.71
B-61.1	394	182	0.48	259	231	0.00119	0.00084	0.01549	0.12687	0.02820	0.56954	0.02313	17.019	1.443	0.21673	0.01506	2905.9	95.7	2956.6	116.8	98.3	1.7	5.92	77	97	85	0.74
B-14.1	516	290	0.58	357	12	0.00005	0.00005	0.00059	0.15667	0.01559	0.58406	0.01001	17.476	0.321	0.21701	0.00103	2965.3	40.9	2958.7	7.7	100.2	-0.2	7.90	54	63	54	0.79
B-48.1	158	73	0.48	108	2	0.00003	0.00010	0.00038	0.12851	0.00970	0.59006	0.03118	17.669	1.378	0.21718	0.01110	2989.7	127.7	2959.9	85.0	101.0	-1.0	2.38	72	88	77	0.75
B-39.1	233	122	0.54	152	13	0.00012	0.00064	0.00157	0.14480	0.02723	0.55794	0.05603	16.729	3.129	0.21746	0.03170	2858.1	236.1	2962.0	257.0	96.5	3.5	3.54	80	111	91	0.77
B-12.2†	88	46	0.54	53	5	0.00013	0.00016	0.00174	0.14795	0.02800	0.51626	0.04009	15.501	1.545	0.21777	0.01167	2683.3	172.7	2964.3	89.1	90.5	9.5	1.34	"	"	"	"
B-43.1	501	324	0.67	358	15	0.00006	0.00002	0.00077	0.17916	0.01415	0.59279	0.04752	17.809	2.116	0.21789	0.01705	3000.7	195.3	2965.2	132.2	101.2	-1.2	7.80	50	87	65	0.70
B-16.1	380	197	0.54	259	4	0.00002	0.00019	0.00028	0.14740	0.01344	0.57984	0.01079	17.483	0.448	0.21868	0.00338	2948.1	44.2	2971.0	25.2	99.2	0.8	5.81	82	122	97	0.78
B-38.1†	243	97	0.41	117	1288	0.01260	0.00053	0.16425	0.14672	0.04354	0.41109	0.01289	12.396	1.132	0.21869	0.01792	2219.9	59.2	2971.1	138.6	74.7	25.3	3.64	70	142	93	0.58
B-63.1	279	161	0.59	192	13	0.00010	0.00022	0.00125	0.16165	0.01110	0.57836	0.03134	17.482	1.624	0.21922	0.01512	2942.1	129.3	2975.0	115.7	98.9	1.1	4.32	97	136	108	0.63
B-12.1	108	61	0.59	73	1	0.00001	0.00001	0.00013	0.15583	0.00736	0.57053	0.01957	17.251	0.858	0.21929	0.00702	2910.0	80.8	2975.5	52.5	97.8	2.2	1.67	60	91	71	0.76
B-62.1†	298	200	0.69	189	898	0.00634	0.00010	0.08246	0.22520	0.02133	0.50852	0.01207	15.416	1.430	0.21988	0.01908	2650.3	51.8	2979.8	147.1	88.9	11.1	4.69	88	148	114	0.67
B-42.1†	586	507	0.89	407	24	0.00009	0.00005	0.00112	0.24510	0.00845	0.54956	0.02036	16.805	0.821	0.22179	0.00611	2823.3	85.3	2993.7	45.0	94.3	5.7	9.56	97	113	100	0.80
B-29.1†	175	72	0.43	49	7	0.00017	0.00020	0.00222	0.04618	0.00754	0.25427	0.00473	7.906	0.212	0.22549	0.00387	1460.5	24.3	3020.3	27.8	48.4	51.6	2.70	52	85	64	0.68
B-8.1	201	107	0.55	137	277	0.00272	0.00024	0.03489	0.15420	0.02143	0.57102	0.04887	18.192	2.547	0.23106	0.02326	2912.0	203.7	3059.4	170.9	95.2	4.8	3.22	57	94	69	0.74
B-49.1	114	57	0.52	81	12	0.00021	0.00007	0.00266	0.13609	0.01551	0.60597	0.06130	19.481	2.926	0.23316	0.02311	3053.9	250.9	3073.9	167.9	99.3	0.7	1.83	71	99	81	0.71
B-34.1†	198	502	2.62	116	187	0.00235	0.00065	0.03007	0.25970	0.02415	0.45447	0.01119	14.645	0.799	0.23371	0.01069	2415.1	49.8	3077.6	75.0	78.5	21.5	4.22	52	83	63	0.73
B-55.1†	154	52	0.35	97	46	0.00063	0.00344	0.00804	0.09548	0.11219	0.55147	0.03510	17.932	4.136	0.23584	0.05044	2831.3	147.5	3092.1	390.3	91.6	8.4	2.43	59	109	77	0.40
B-36.1	236	202	0.89	188	17	0.00013	0.00015	0.00167	0.23427	0.01653	0.62757	0.04168	20.424	2.043	0.23603	0.01580	3140.0	167.2	3093.4	111.0	101.5	-1.5	4.05	82	130	100	0.80
B-46.1	91	47	0.53	68	2	0.00005	0.00065	0.00063	0.13942	0.02196	0.62819	0.06018	20.456	2.232	0.23617	0.00983	3142.4	242.8	3094.3	68.0	101.6	-1.6	1.48	66	121	89	0.69
B-41.1	192	133	0.71	146	324	0.00307	0.00019	0.03896	0.19171	0.00730	0.61584	0.01416	20.311	0.586	0.23920	0.00353	3093.3	56.8	3114.7	23.7	99.3	0.7	3.25	62	93	76	0.78
B-64.1	55	28	0.53	39	12	0.00043	0.00119	0.00541	0.13905	0.03886	0.60228	0.04207	19.996	2.249	0.24080	0.01923	3039.0	171.5	3125.2	133.2	97.2	2.8	0.90	93	153	113	0.75
B-21.1	101	73	0.75	78	13	0.00025	0.00058	0.00319	0.21218	0.02932	0.61318	0.04090	20.447	1.627	0.24184	0.00867	3082.7	165.6	3132.1	58.2	98.4	1.6	1.73	60	97	74	0.75
B-60.1†	168	79	0.49	102	955	0.01093	0.00097	0.13838	0.10328	0.05162	0.52441	0.04749	17.563	4.474	0.24290	0.05515	2717.9	204.0	3139.0	416.6	86.6	13.4	2.77	72	100	82	0.71
B-19.1	200	43	0.22	140	8	0.00008	0.00045	0.00096	0.05857	0.01485	0.62584	0.01220	21.012	0.833	0.24350	0.00783	3133.1	48.6	3143.0	52.0	99.7	0.3	3.18	57	97	72	0.75
B-9.1	77	42	0.56	59	0	0.00001	0.00001	0.00013	0.15326	0.01436	0.63037	0.01281	21.257	0.513	0.24457	0.00263	3151.1	50.8	3150.0	17.2	100.0	0.0	1.29	85	138	107	0.73
B-54.1	151	94	0.64	110	86	0.00110	0.00015	0.01386	0.17243	0.01998	0.59536	0.04956	20.117	2.557	0.24507	0.02112	3011.1	203.4	3153.2	143.9	95.5	4.5	2.57	66	107	83	0.72
B-53.1	104	49	0.48	74	4	0.00008	0.00035	0.00098	0.11999	0.01270	0.60192	0.03360	20.353	1.541	0.24523	0.01095	3037.6	136.6	3154.2	72.7	96.3	3.7	1.74	60	112	79	0.68
B-28.1	107	85	0.81	86	7	0.00012	0.00010	0.00156	0.21910	0.05446	0.63110	0.03942	21.411	1.939	0.24605	0.01432	3154.0	157.7	3159.5	95.5	99.8	0.2	1.88	49	100	66	0.66
B-58.1	88	50	0.59	67	10	0.00022	0.00242	0.00278	0.15539	0.07873	0.62440	0.04043	21.206	3.650	0.24631	0.03734	3127.4	162.5	3161.2	263.6	98.9	1.1	1.50	67	124	87	0.72
B-5.1	262	162	0.64	198	113	0.00080	0.00019	0.01010	0.16094	0.01565	0.62200	0.04759	21.221	2.463	0.24744	0.01936	3117.9	192.0	3168.5	129.9	98.4	1.6	4.50	62	108	79	0.74
B-27.1	104	44	0.43	77	1	0.00001	0.00001	0.00013	0.11589	0.00163	0.62554	0.02631	21.517	0.988	0.24947	0.00346	3131.9	105.2	3181.4	22.1	98.4	1.6	1.74	49	97	68	0.72
B-57.1	203	82	0.42	154	10	0.00009	0.00081	0.00109	0.11198	0.02680	0.64668	0.04053	22.297	2.249	0.25006	0.01790	3215.2	160.7	3185.2	118.2	100.9	-0.9	3.39	61	109	78	0.71
B-20.1	248	126	0.52	192	7	0.00005	0.00005	0.00062	0.14012	0.01486	0.64419	0.06702	22.313	3.469	0.25121	0.02594	3205.5	268.3	3192.4	173.7	100.4	-0.4	4.23	69	87	75	0.77
B-56.1	130	66	0.53	97	13	0.00018	0.00112	0.00230	0.14250	0.03634	0.62301	0.01671	21.732	1.593	0.25299	0.01643	3121.9	66.7	3203.6	106.6	97.4	2.6	2.23	54	98	71	0.66
B-11.1†	171	72	0.44	122	51	0.00057	0.00015	0.00717	0.12288	0.01414	0.60162	0.05685	21.055	3.085	0.25382	0.02559	3036.4	233.0	3208.8	169.1	94.6	5.4	2.90	65	88	73	0.72
B-40.1	13	6	0.43	10	2	0.00022	0.00091	0.00280	0.12651	0.03270	0.63893	0.03069	22.510	1.780	0.25551	0.01458	3184.8	121.9	3219.3	93.1	98.9	1.1	0.23	54	66	57	0.80
B-23.1	226	125	0.57	178	15	0.00012	0.00009	0.00153	0.15904	0.01017	0.64609	0.03814	22.861	2.019	0.25663	0.01508	3212.9	151.1	3226.1	95.9	99.6	0.4	3.94	60	77	68	0.81
B-51.1†	215	197	0.95	92	5	0.00008	0.00036	0.00104	0.25534	0.01428	0.32719	0.01154	11.932	0.639	0.26449	0.00956	1824.7	56.3	3273.7	58.0	55.7	44.3	4.06	74	116	86	0.51
B-7.1	119	79	0.69	98	4	0.00006	0.00004	0.00073	0.19145	0.00219	0.65254	0.01479	24.787	1.069	0.27550	0.00935	3238.1	57.9	3337.6	54.1	97.0	3.0	2.24	75	83	73	0.70
B-66.1	381	56	0.15	294	18	0.00008	0.00026	0.00097	0.03861	0.00830	0.68128	0.01115	26.154	1.561	0.27843	0.01542	3349.3	42.9	3354.1	89.3	99.9	0.1	6.66	89	115	102	0.73
B-50.1	361	346	0.99	329	7	0.00003	0.00002	0.00039	0.26077	0.00216	0.68299	0.01212	26.932	0.629	0.28600	0.00375	3355.8	46.6	3396.0	20.6	98.8	1.2	7.28	62	102	77	0.67
B-44.1	178	46	0.27	137	76	0.00075	0.00015	0.00905	0.06751	0.00883	0.66045	0.03460	26.049	2.238	0.28606	0.01769	3268.9	135.7	3396.3	99.8	96.2	3.8	3.23	69	111	86	0.75
B-30.1	159	81	0.52	130	107	0.00117	0.00015	0.01405	0.14363	0.02039	0.65983	0.10675	26.286	4.366	0.28893	0.00648	3266.5	428.5	3411.9	35.3	95.7	4.3	3.03	55	66	55	0.58
B-33.1	809	68	0.09	626	74	0.00016	0.00003	0.00187	0.02215	0.00352	0.68457	0.08558	27.639	5.178	0.29283	0.03653	3361.9	336.1	3432.7	208.6	97.9	2.1	14.55	76	128	96	0.75
B-37.1	396	376	0.98	382	55	0.00022	0.00128	0.00265	0.25355	0.04141	0.72151	0.03003	29.746	2.473	0.29901	0.02002	3501.7	113.5	3465.1	107.8	101.1	-1.1	8.24	58	107	76	0.70
B-26.2R	189	84	0.46	159	615	0.00524	0.00031	0.06223	0.13796	0.01581	0.67860	0.02449	28.124	1.194	0.30058	0.00551	3339.0	94.8	3473.2	28.7	96.1	3.9	3.67	"	"	"	"
B-52.1	486	230	0.49	427	717	0.00237	0.00021	0.02798	0.13941	0.01965	0.70697	0.06304	29.758	4.112	0.30528	0.02900	3447.0	242.6	3497.2	155.2	98.6	1.4	9.59	60	106	78	0.65
B-31.1	47	27	0.58	42	9	0.00033	0.00031	0.00385	0.14530	0.01010	0.71290	0.01501	30.139	1.062	0.30662	0.00789	3469.4	56.7	3504.0	40.4	99.0	1.0	0.95	70	97	77	0.75
B-13.1†	177	63	0.36	136	51	0.00053	0.00006	0.00628	0.10609	0.00474	0.63310	0.02030	26.810	2.731	0.30713	0.02848	3161.8	80.7	3506.6	151.2	90.2	9.8	3.45	65	103	79	0.75
B-18.1	181	83	0.47	163	160	0.00139	0.00072	0.01623	0.12083	0.02677	0.72873	0.06132	31.883	4.210	0.31731	0.02912	3528.7	232.8	3556.9	149.0	99.2	0.8	3.67	63	106	81	0.74
B-22.1	323	23	0.07	277	3	0.00001	0.00008	0.00015	0.01976	0.00272	0.74189	0.04893	32.820	6.220	0.32085	0.05442	3577.6	183.7	3573.9	288.8	100.1	-0.1	6.23	56	64	58	0.82
B-2.1	156	184	1.21	166	6	0.00006	0.00002	0.00073	0.31849	0.00662	0.75172	0.01400	33.289	0.670	0.32118	0.00180	3613.8	51.7	3575.5	8.6	101.1	-1.1	3.54	55	92	67	0.71
B-32.1†	689	455	0.68	451	11	0.00004	0.00008	0.00041	0.13560	0.01239	0.52187	0.04473	23.242	3.082	0.32301	0.02941	2707.1	192.3	3584.2	147.4	75.5	24.5	14.57	53	127	84	0.61
B-15.1	116	61	0.54	113	1	0.00001	0.00001	0.00012	0.14104	0.00251	0.77201	0.01711	35.008	0.994	0.32888	0.00500	3688.1	62.5	3611.9	23.5	102.1	-2.1	2.44	60	108	81	0.71
B-6.1	60	13	0.22	55	4	0.00009	0.00012	0.00108	0.06156	0.00415	0.76208	0.01319	35.128	0.731	0.33431	0.00320	3651.9	48.4	3637.0	14.7	100.4	-0.4	1.23	64	87	69	0.72
B-35.1	181	101	0.58	177	49	0.00042	0.00020	0.00475	0.16440	0.01169	0.75495	0.10548	35.404	5.080	0.34012	0.00667	3625.7	399.6	3663.3	30.3	99.0	1.0	3.92	71	82	73	0.78
B-65.1	70	0	0.01	61	11	0.00024	0.00052	0.00274	-0.00311	0.01670	0.75307	0.03885	37.402	2.794	0.36021	0.01728	3618.8	144.5	3750.7	74.9	96.5	3.5	1.46	90	117	99	0.76
B-45.1	107	62	0.60	111	13	0.00018	0.00010	0.00199	0.15445	0.00522	0.79589	0.02924	40.353	2.069	0.36772	0.01157	3774.4	105.8	3782.1	48.5	99.8	0.2	2.46	69	105	84	0.64
B-25.1	115	113	1.02	140	9	0.00011	0.00052	0.00113	0.25633	0.01644	0.84582	0.02531	48.858	1.835	0.41894	0.00807	3951.2	89.0	3978.5	29.2	99.3	0.7	3.08	66	82	71	0.82

Dwyer Lake Quartzite, Slave Province, Magnetic Fraction 'C' 1.8A 5°M

																	Apparent Ages (Ma)										
Spot name	U (ppm)	Th (ppm)	Th/U	Pb (ppm)	204Pb (ppb)	204Pb/ 206Pb	±204Pb/ 206Pb	f206	208Pb/ 206Pb	±208Pb/ 206Pb	206Pb/ 238U	±206Pb/ 238U	207Pb/ 235U	±207Pb/ 235U	207Pb/ 206Pb	±207Pb/ 206Pb	206Pb/ 238U	±206Pb/ 238U	207Pb/ 206Pb	±207Pb/ 206Pb	Conc.%	Disc.%	a-dose events/mg x 10^15	Breadth µm	Length µm	EqDiam µm	Form Factor
C-33.1†	398	196	0.51	189	830	0.00568	0.00038	0.07503	0.18498	0.03367	0.39589	0.00674	11.392	0.421	0.20870	0.00641	2150.1	31.2	2895.5	50.7	74.3	25.7	5.84	66	89	76	0.73
C-8.1	133	64	0.50	90	10	0.00014	0.00018	0.00189	0.13596	0.02550	0.58087	0.06651	16.919	2.869	0.21124	0.02358	2952.3	277.1	2915.1	193.3	101.3	-1.3	1.97	88	109	94	0.83
C-28.1†	479	191	0.41	293	7	0.00003	0.00019	0.00045	0.11319	0.01128	0.53616	0.04706	15.627	2.031	0.21139	0.01808	2767.3	200.6	2916.3	145.7	94.9	5.1	6.98	79	102	85	0.77
C-40.1	109	100	0.95	78	5	0.00009	0.00102	0.00123	0.25419	0.05779	0.56812	0.09470	16.583	4.362	0.21169	0.03889	2900.1	401.6	2918.6	333.5	99.4	0.6	1.72	84	117	96	0.77
C-25.1†	342	189	0.57	217	899	0.00530	0.00011	0.06955	0.15256	0.00680	0.53913	0.01071	15.840	0.405	0.21309	0.00294	2779.8	45.0	2929.2	22.5	94.9	5.1	5.14	96	125	104	0.71
C-38.1	515	297	0.59	350	13	0.00005	0.00002	0.00065	0.16690	0.06547	0.57213	0.02477	16.837	1.022	0.21344	0.00800	2916.6	102.4	2931.8	62.0	99.5	0.5	7.79	71	90	76	0.78
C-11.1†	556	275	0.51	297	12	0.00005	0.00002	0.00070	0.16260	0.01520	0.45020	0.01496	13.257	0.517	0.21357	0.00356	2396.2	66.8	2932.9	27.2	81.7	18.3	8.31	61	91	74	0.82
C-59.1	566	465	0.85	416	24	0.00008	0.00023	0.00109	0.23648	0.00951	0.58834	0.01675	17.409	0.786	0.21460	0.00680	2982.7	68.3	2940.6	52.2	101.4	-1.4	8.94	57	77	64	0.82
C-5.1	425	71	0.17	274	9	0.00004	0.00023	0.00053	0.05158	0.00748	0.59202	0.02887	17.595	0.950	0.21555	0.00386	2997.6	118.0	2947.7	29.2	101.7	-1.7	6.05	59	73	62	0.81
C-18.1	319	216	0.70	225	5	0.00003	0.00002	0.00039	0.19142	0.02826	0.58206	0.08580	17.304	4.359	0.21561	0.04025	2957.2	359.5	2948.2	338.8	100.3	-0.3	4.94	83	121	95	0.79
C-39.1	389	263	0.70	275	9	0.00005	0.00018	0.00060	0.19420	0.06176	0.58238	0.05178	17.318	2.313	0.21566	0.01923	2958.5	214.5	2948.6	151.8	100.3	-0.3	6.03	55	76	60	0.77
C-9.1	520	286	0.57	355	6	0.00002	0.00000	0.00032	0.15774	0.00291	0.57756	0.01060	17.176	0.359	0.21568	0.00172	2938.8	43.5	2948.7	13.0	99.7	0.3	7.90	68	95	77	0.56
C-47.1	422	273	0.67	283	7	0.00004	0.00002	0.00047	0.17961	0.02334	0.55852	0.07196	16.668	3.402	0.21644	0.03095	2860.5	304.7	2954.4	251.8	96.8	3.2	6.53	79	102	89	0.79
C-21.1	378	165	0.45	250	117	0.00062	0.00025	0.00812	0.12086	0.01037	0.57370	0.02550	17.146	1.171	0.21676	0.01010	2923.0	105.3	2956.8	77.3	98.9	1.1	5.67	70	101	81	0.78
C-27.1	267	231	0.90	191	48	0.00037	0.00006	0.00482	0.25109	0.02889	0.56453	0.04553	16.878	2.074	0.21684	0.01804	2885.3	190.4	2957.4	141.0	97.6	2.4	4.28	50	87	59	0.68
C-57.1	317	235	0.77	227	7	0.00004	0.00000	0.00054	0.20738	0.02277	0.58475	0.05959	17.497	2.785	0.21701	0.02392	2968.1	247.1	2958.7	189.9	100.3	-0.3	4.98	79	110	90	0.79
C-52.1†	236	99	0.43	145	62	0.00057	0.00009	0.00741	0.12127	0.02807	0.53271	0.05587	15.956	2.583	0.21723	0.02409	2752.9	239.4	2960.3	191.1	93.0	7.0	3.53	77	98	81	0.74
C-3.1	441	596	1.40	354	9	0.00004	0.00015	0.00056	0.38149	0.03207	0.58248	0.03270	17.447	1.458	0.21724	0.01202	2958.8	134.6	2960.4	92.2	99.9	0.1	7.61	76	148	104	0.70
C-34.1	317	91	0.30	211	14	0.00009	0.00033	0.00117	0.08073	0.01477	0.59460	0.08106	17.819	3.456	0.21735	0.02650	3008.0	336.3	2961.2	211.7	101.6	-1.6	4.65	110	147	118	0.73
C-46.1	271	145	0.55	186	1	0.00001	0.00002	0.00009	0.14330	0.00211	0.58677	0.01010	17.606	0.775	0.21761	0.00836	2976.3	41.2	2963.1	63.4	100.4	-0.4	4.14	62	78	66	0.75
C-16.1	441	266	0.62	317	20	0.00009	0.00002	0.00115	0.17238	0.00372	0.60041	0.03785	18.035	1.208	0.21785	0.00349	3031.5	154.3	2964.9	26.1	102.2	-2.2	6.81	98	197	138	0.71
C-17.1	447	167	0.39	293	10	0.00005	0.00008	0.00062	0.10313	0.01433	0.57617	0.07494	17.310	3.368	0.21789	0.02819	2933.1	314.0	2965.2	225.6	98.9	1.1	6.66	79	117	88	0.68
C-31.1†	476	109	0.24	275	2526	0.01039	0.00062	0.13552	0.08394	0.03396	0.51559	0.03218	15.503	1.961	0.21807	0.02234	2680.4	138.4	2966.5	175.6	90.4	9.6	6.92	86	105	93	0.79
C-19.1	326	219	0.69	234	13	0.00008	0.00079	0.00103	0.19255	0.02609	0.59124	0.02036	17.779	1.198	0.21809	0.01173	2994.5	83.0	2966.7	89.4	100.9	-0.9	5.09	63	78	70	0.82
C-4.1†	456	81	0.18	241	769	0.00388	0.00092	0.05065	0.05766	0.04197	0.48125	0.07359	14.474	3.708	0.21814	0.04086	2532.7	328.5	2967.0	339.4	85.4	14.6	6.57	66	153	96	0.58
C-2.1	202	106	0.54	134	4	0.00004	0.00015	0.00052	0.14050	0.00502	0.56670	0.01252	17.093	0.487	0.21876	0.00339	2894.3	51.7	2971.6	25.2	97.4	2.6	3.09	76	141	104	0.71
C-35.1	90	81	0.93	64	13	0.00030	0.00013	0.00388	0.25614	0.01022	0.56090	0.01108	16.918	0.441	0.21876	0.00321	2870.4	45.9	2971.6	23.9	96.6	3.4	1.46	63	79	68	0.79
C-14.1†	199	105	0.55	127	162	0.00176	0.00044	0.02288	0.17403	0.02310	0.53157	0.03398	16.037	1.667	0.21881	0.01628	2748.0	144.6	2971.9	125.3	92.5	7.5	3.04	105	161	126	0.79
C-41.1	556	283	0.53	373	12	0.00004	0.00025	0.00058	0.13536	0.02561	0.57499	0.10222	17.349	4.683	0.21883	0.03985	2928.3	432.6	2972.1	328.7	98.5	1.5	8.49	80	122	90	0.71
C-61.1	270	117	0.45	177	318	0.00236	0.00018	0.03078	0.13266	0.00674	0.56363	0.01212	17.022	0.494	0.21904	0.00371	2881.6	50.2	2973.6	27.6	96.9	3.1	4.08	55	83	68	0.76
C-55.1†	564	366	0.67	360	359	0.00140	0.00051	0.01825	0.20697	0.08016	0.51996	0.17301	15.827	8.060	0.22077	0.07642	2699.0	779.0	2986.3	706.3	90.4	9.6	8.87	79	148	105	0.74
C-29.1†	680	257	0.39	225	82	0.00051	0.00006	0.00659	0.17832	0.01867	0.27420	0.02659	8.382	1.229	0.22171	0.02184	1562.1	136.0	2993.1	168.0	52.2	47.8	10.27	65	114	85	0.77
C-50.1	111	50	0.46	74	8	0.00015	0.00006	0.00190	0.13337	0.05219	0.56864	0.09734	17.529	4.387	0.22358	0.03631	2902.2	413.0	3006.6	288.3	96.5	3.5	1.71	83	131	101	0.72
C-45.1†	123	120	1.01	79	59	0.00115	0.00015	0.01476	0.31135	0.02242	0.48075	0.02634	15.164	1.025	0.22876	0.00761	2530.5	115.7	3043.4	54.3	83.1	16.9	2.10	64	121	84	0.71
C-7.1	126	104	0.85	97	4	0.00005	0.00028	0.00069	0.22646	0.03946	0.60702	0.08899	19.978	5.059	0.23869	0.04511	3058.1	367.2	3111.3	338.5	98.3	1.7	2.17	64	102	76	0.72
C-6.1	109	58	0.55	79	2	0.00004	0.00023	0.00053	0.15435	0.03029	0.60640	0.05576	20.129	2.771	0.24075	0.02205	3055.6	227.7	3124.9	153.8	97.8	2.2	1.80	82	126	97	0.79
C-60.1‡	597	165	0.29	455	34	0.00010	0.00038	0.00125	0.07314	0.01271	0.67190	0.02229	22.634	1.012	0.24432	0.00637	3313.2	86.5	3148.3	42.1	105.2	-5.2	9.60	102	132	112	0.72
C-51.1	120	57	0.49	86	123	0.00190	0.00029	0.02389	0.10736	0.03066	0.61572	0.06607	20.897	3.491	0.24615	0.02838	3092.9	269.2	3160.2	195.9	97.9	2.1	2.01	66	97	74	0.72
C-62.1	797	468	0.61	642	19	0.00004	0.00017	0.00053	0.16357	0.02207	0.66245	0.08499	22.662	4.519	0.24811	0.03411	3276.7	338.3	3172.8	236.7	103.3	-3.3	13.63	82	103	90	0.81
C-43.1	125	112	0.93	104	13	0.00018	0.00004	0.00229	0.26411	0.01416	0.63833	0.03492	22.038	1.777	0.25039	0.01321	3182.5	138.9	3187.2	86.1	99.9	0.1	2.26	81	97	84	0.76
C-30.1	265	156	0.61	197	823	0.00553	0.00017	0.06925	0.16140	0.01546	0.61061	0.01332	21.183	0.635	0.25161	0.00453	3072.4	53.6	3194.9	28.8	96.2	3.8	4.58	62	75	62	0.59
C-24.1	191	41	0.22	128	24	0.00024	0.00084	0.00302	0.04174	0.02727	0.60192	0.03977	20.900	2.310	0.25183	0.02033	3037.6	162.1	3196.3	133.9	95.0	5.0	3.12	100	115	102	0.78
C-10.1†	362	135	0.39	243	101	0.00057	0.00009	0.00711	0.11885	0.00676	0.56934	0.01958	19.836	0.988	0.25269	0.00808	2905.1	80.9	3201.7	51.5	90.7	9.3	6.07	72	101	86	0.75
C-22.1†	112	86	0.79	70	14	0.00030	0.00028	0.00376	0.24811	0.01482	0.48368	0.01043	16.959	0.560	0.25429	0.00571	2543.3	45.5	3211.7	35.9	79.2	20.8	2.00	72	110	84	0.69
C-36.1†	454	637	1.45	125	124	0.00155	0.00017	0.01890	0.29639	0.01071	0.20302	0.00649	7.636	0.359	0.27278	0.00836	1191.5	34.9	3322.1	48.9	35.9	64.1	9.39	63	110	80	0.77
C-58.1	193	103	0.55	165	172	0.00147	0.00002	0.01785	0.14703	0.05454	0.69366	0.01577	26.944	0.815	0.28172	0.00488	3396.6	60.3	3372.5	27.3	100.7	-0.7	3.61	72	120	89	0.70
C-23.1	622	259	0.43	526	91	0.00024	0.00008	0.00294	0.11369	0.00859	0.70356	0.01708	27.411	0.858	0.28257	0.00479	3434.1	65.0	3377.2	26.7	101.7	-1.7	11.46	60	85	69	0.74
C-63.1	329	222	0.70	289	7	0.00004	0.00041	0.00042	0.18216	0.01372	0.69436	0.01975	27.499	1.238	0.28723	0.00906	3399.2	75.6	3402.7	50.0	99.9	0.1	6.39	88	141	109	0.74
C-37.1	563	284	0.52	472	20	0.00006	0.00018	0.00074	0.13919	0.00947	0.68259	0.03749	27.073	2.258	0.28766	0.01619	3354.3	145.2	3405.0	90.5	98.5	1.5	10.67	103	132	110	0.69
C-49.1	457	73	0.16	364	18	0.00007	0.00024	0.00081	0.04071	0.00793	0.69481	0.01507	27.684	0.831	0.28897	0.00526	3400.9	57.6	3412.1	28.6	99.7	0.3	8.24	75	96	79	0.71
C-20.1	134	45	0.35	106	63	0.00081	0.00009	0.00971	0.09116	0.01687	0.66459	0.04803	26.774	3.601	0.29219	0.03061	3284.9	188.8	3429.3	173.1	95.8	4.2	2.51	52	105	72	0.67
C-32.2R†	146	39	0.27	79	151	0.00263	0.00023	0.03133	0.11268	0.01121	0.44351	0.02868	18.094	1.547	0.29589	0.01432	2366.3	129.4	3448.8	77.2	68.6	31.4	2.73	"	"	"	"
C-54.1	300	288	0.99	287	9	0.00005	0.00020	0.00060	0.27683	0.05829	0.70466	0.14688	29.312	9.196	0.30169	0.06331	3438.3	580.8	3478.9	369.7	98.8	1.2	6.29	58	123	83	0.71
C-56.1†	197	179	0.94	164	26	0.00024	0.00007	0.00276	0.17424	0.04437	0.64957	0.04413	28.133	2.462	0.31411	0.01487	3226.5	174.8	3541.2	74.9	91.1	8.9	4.22	55	65	57	0.81
C-12.1	141	75	0.55	136	79	0.00084	0.00010	0.00987	0.13798	0.01496	0.76788	0.07227	33.541	4.236	0.31679	0.02322	3673.1	269.1	3554.3	117.7	103.3	-3.3	2.89	59	77	64	0.80
C-48.1	133	58	0.45	123	9	0.00010	0.00009	0.00117	0.12095	0.01660	0.74605	0.09840	32.654	6.443	0.31744	0.04165	3593.0	373.9	3557.5	218.2	101.0	-1.0	2.69	97	115	99	0.59
C-53.1†	507	333	0.68	403	677	0.00249	0.00043	0.02903	0.20051	0.04804	0.60786	0.10280	26.702	7.199	0.31860	0.06050	3061.4	425.9	3563.1	327.9	85.9	14.1	10.61	67	111	80	0.71
C-44.1	231	207	0.93	226	120	0.00083	0.00007	0.00962	0.24540	0.03730	0.72310	0.03903	32.342	3.350	0.32439	0.02657	3507.7	147.7	3590.8	131.9	97.7	2.3	5.06	62	115	84	0.64
C-42.1†	304	71	0.24	222	9	0.00006	0.00003	0.00065	0.06462	0.01349	0.60909	0.10517	27.257	7.603	0.32456	0.06445	3066.4	435.7	3591.6	344.2	85.4	14.6	6.07	76	97	86	0.83
C-32.1	275	99	0.37	253	12	0.00007	0.00015	0.00078	0.09742	0.01420	0.74980	0.09480	33.914	6.385	0.32804	0.04087	3606.8	359.1	3608.0	205.6	100.0	0.0	5.64	67	84	70	0.73
C-26.1†	78	45	0.60	73	28	0.00057	0.00095	0.00639	0.14230	0.03097	0.73137	0.03054	35.784	2.317	0.35486	0.01580	3538.5	114.7	3728.0	69.5	94.9	5.1	1.75	69	97	78	0.74
C-13.1	247	170	0.71	276	9	0.00005	0.00020	0.00056	0.18336	0.00657	0.82918	0.01789	43.828	1.498	0.38335	0.00918	3892.8	63.4	3845.0	36.6	101.2	-1.2	5.96	82	143	106	0.77
C-15.1	343	288	0.87	414	12	0.00005	0.00007	0.00052	0.21610	0.00982	0.86182	0.04854	49.020	3.750	0.41253	0.01865	4006.8	170.3	3955.4	69.5	101.3	-1.3	8.90	69	147	101	0.67
C-1.1	269	77	0.29	290	2	0.00001	0.00008	0.00011	0.10662	0.00315	0.81883	0.02197	47.328	2.139	0.41920	0.01390	3856.2	78.3	3979.4	50.6	96.9	3.1	6.58	69	132	93	0.76

Dwyer Lake Quartzite, Slave Province, Magnetic Fraction 'D' 1.8A 10°M

																	Apparent Ages (Ma)										
Spot name	U (ppm)	Th (ppm)	Th/U	Pb (ppm)	204Pb (ppb)	204Pb/ 206Pb	±204Pb/ 206Pb	f206	208Pb/ 206Pb	±208Pb/ 206Pb	206Pb/ 238U	±206Pb/ 238U	207Pb/ 235U	±207Pb/ 235U	207Pb/ 206Pb	±207Pb/ 206Pb	206Pb/ 238U	±206Pb/ 238U	207Pb/ 206Pb	±207Pb/ 206Pb	Conc.%	Disc.%	a-dose events/mg x 10^15	Breadth µm	Length µm	EqDiam µm	Form Factor
D-46.1†	1524	883	0.60	736	4118	0.00694	0.00011	0.09364	0.17083	0.00521	0.41168	0.02913	10.964	1.165	0.19316	0.01371	2222.6	134.4	2769.3	121.4	80.3	19.7	21.22	62	108	81	0.76
D-33.1	743	375	0.52	474	390	0.00110	0.00016	0.01455	0.14337	0.02191	0.54907	0.06580	15.733	3.119	0.20782	0.02986	2821.3	279.8	2888.6	254.7	97.7	2.3	10.87	54	103	71	0.72
D-5.1†	314	169	0.56	188	620	0.00429	0.00030	0.05650	0.16290	0.01158	0.50636	0.00972	14.710	0.507	0.21070	0.00554	2641.1	41.7	2910.9	43.2	90.7	9.3	4.67	61	82	66	0.75
D-48.1†	388	353	0.94	197	195	0.00141	0.00013	0.01856	0.23224	0.02504	0.40862	0.03735	11.884	1.682	0.21093	0.02052	2208.6	173.2	2912.7	167.0	75.8	24.2	6.12	75	120	93	0.79
D-37.1	1099	485	0.46	683	34	0.00007	0.00004	0.00089	0.12218	0.00942	0.54099	0.04146	15.834	1.805	0.21228	0.01600	2787.6	175.8	2923.0	127.5	95.4	4.6	16.19	67	111	85	0.78
D-9.1	839	411	0.51	548	32	0.00008	0.00005	0.00102	0.13593	0.00251	0.56303	0.01048	16.486	0.945	0.21237	0.01103	2879.1	43.4	2923.7	86.6	98.5	1.5	12.46	65	96	75	0.71
D-24.1†	400	570	1.47	270	45	0.00027	0.00005	0.00350	0.39698	0.01809	0.48615	0.02238	14.251	0.962	0.21260	0.00935	2554.0	97.8	2925.5	73.0	87.3	12.7	6.85	77	91	78	0.75
D-50.1†	349	290	0.86	218	33	0.00022	0.00014	0.00287	0.23351	0.01757	0.50019	0.03611	14.695	1.594	0.21308	0.01544	2614.6	157.1	2929.1	122.3	89.3	10.7	5.49	72	118	91	0.79
D-15.1†	516	722	1.44	320	140	0.00071	0.00037	0.00928	0.40436	0.01281	0.44477	0.01483	13.085	0.596	0.21338	0.00578	2372.0	66.5	2931.4	44.5	80.9	19.1	8.84	97	128	104	0.61
D-23.1†	388	169	0.45	214	259	0.00158	0.00187	0.02071	0.11253	0.06277	0.48300	0.04180	14.214	2.536	0.21344	0.03108	2540.3	184.3	2931.8	257.4	86.6	13.4	5.74	69	108	84	0.76
D-3.1	971	269	0.29	641	14	0.00003	0.00014	0.00038	0.07822	0.00473	0.59396	0.00973	17.484	0.366	0.21350	0.00239	3005.4	39.5	2932.3	18.2	102.5	-2.5	13.99	75	98	79	0.59
D-34.1	219	79	0.37	139	11	0.00011	0.00026	0.00141	0.10550	0.01019	0.55979	0.01648	16.535	0.750	0.21422	0.00665	2865.8	68.5	2937.8	51.1	97.5	2.5	3.21	82	117	96	0.74
D-58.1	508	224	0.46	328	48	0.00019	0.00008	0.00255	0.12124	0.01544	0.56139	0.01005	16.600	0.378	0.21446	0.00258	2872.4	41.6	2939.6	19.6	97.7	2.3	7.55	68	160	106	0.60
D-18.1†	411	243	0.61	259	383	0.00201	0.00016	0.02635	0.17811	0.04050	0.52528	0.04257	15.602	2.049	0.21542	0.02018	2721.5	182.5	2946.8	160.0	92.4	7.6	6.29	60	84	68	0.76
D-54.1	491	344	0.72	341	63	0.00026	0.00033	0.00343	0.20021	0.02117	0.57028	0.04128	16.940	1.875	0.21543	0.01619	2909.0	171.7	2946.9	126.9	98.7	1.3	7.63	73	144	100	0.70
D-12.1†	294	192	0.67	190	56	0.00041	0.00013	0.00539	0.18345	0.00940	0.53609	0.02882	15.945	2.175	0.21572	0.02564	2767.1	122.1	2949.0	206.1	93.8	6.2	4.54	90	129	106	0.76
D-20.1	770	363	0.49	514	13	0.00003	0.00007	0.00045	0.13514	0.00345	0.57393	0.01270	17.072	0.573	0.21573	0.00487	2923.9	52.2	2949.1	36.9	99.1	0.9	11.55	60	99	76	0.76
D-10.1	425	342	0.83	295	10	0.00005	0.00000	0.00063	0.22554	0.03318	0.55934	0.04715	16.651	2.086	0.21590	0.01787	2863.9	197.9	2950.4	140.3	97.1	2.9	6.72	101	203	138	0.62
D-6.1	517	322	0.64	342	18	0.00007	0.00018	0.00093	0.17067	0.00817	0.55446	0.02250	16.513	0.959	0.21600	0.00794	2843.7	94.0	2951.1	60.7	96.4	3.6	7.95	59	95	72	0.47
D-19.1	139	50	0.38	90	5	0.00007	0.00079	0.00092	0.10325	0.03575	0.57316	0.01978	17.070	1.301	0.21600	0.01377	2920.8	81.6	2951.1	106.9	99.0	1.0	2.05	76	173	115	0.41
D-45.1	259	124	0.49	168	17	0.00014	0.00030	0.00179	0.13237	0.01109	0.55948	0.01181	16.670	0.539	0.21610	0.00476	2864.5	49.0	2951.8	36.0	97.0	3.0	3.90	86	101	92	0.83
D-2.1	921	567	0.64	649	24	0.00005	0.00002	0.00067	0.17187	0.00297	0.59005	0.01723	17.616	0.584	0.21653	0.00271	2989.6	70.2	2955.1	20.3	101.2	-1.2	14.18	64	139	94	0.56
D-47.1†	523	263	0.52	318	12	0.00005	0.00008	0.00064	0.14017	0.00420	0.52034	0.01569	15.537	0.646	0.21656	0.00544	2700.6	66.9	2955.3	41.1	91.4	8.6	7.91	76	107	87	0.74
D-16.1	413	221	0.55	278	2	0.00001	0.00001	0.00013	0.15158	0.01013	0.57274	0.04018	17.135	1.758	0.21698	0.01445	2919.1	166.8	2958.4	111.7	98.7	1.3	6.28	64	81	68	0.74
D-35.1	188	132	0.72	129	13	0.00014	0.00011	0.00186	0.19033	0.00746	0.56696	0.01958	16.988	0.940	0.21732	0.00851	2895.3	81.1	2960.9	64.6	97.8	2.2	2.94	73	101	84	0.78
D-38.1	431	280	0.67	297	3	0.00002	0.00002	0.00020	0.18137	0.01965	0.57279	0.06374	17.189	2.845	0.21764	0.02381	2919.3	266.7	2963.4	188.4	98.5	1.5	6.70	68	99	76	0.75
D-49.1	572	355	0.64	399	25	0.00009	0.00004	0.00112	0.16721	0.00499	0.58422	0.01832	17.545	0.760	0.21781	0.00571	2966.0	75.0	2964.6	42.9	100.0	0.0	8.86	69	110	83	0.74
D-30.1†	476	482	1.05	327	1057	0.00457	0.00094	0.05960	0.27551	0.07793	0.53294	0.01217	16.006	1.180	0.21783	0.01466	2753.8	51.4	2964.7	112.9	92.9	7.1	7.84	72	83	76	0.87
D-57.1†	706	268	0.39	428	34	0.00010	0.00002	0.00136	0.10293	0.00677	0.53282	0.02659	16.022	1.189	0.21809	0.01070	2753.3	112.8	2966.7	81.4	92.8	7.2	10.53	63	95	77	0.78
D-4.1	623	167	0.28	400	77	0.00025	0.00004	0.00324	0.07073	0.00179	0.57964	0.01261	17.435	0.498	0.21815	0.00349	2947.3	51.7	2967.1	26.0	99.3	0.7	9.12	40	84	58	0.65
D-62.1	252	128	0.53	166	10	0.00008	0.00008	0.00104	0.14291	0.00667	0.56090	0.01317	16.934	0.655	0.21896	0.00613	2870.3	54.6	2973.1	45.8	96.5	3.5	3.85	96	112	97	0.70
D-21.1	514	400	0.80	377	15	0.00006	0.00003	0.00075	0.21297	0.02310	0.59532	0.02766	17.989	2.127	0.21916	0.02259	3011.0	112.8	2974.5	176.6	101.2	-1.2	8.20	69	88	73	0.73
D-59.1	355	192	0.56	231	67	0.00040	0.00035	0.00522	0.15450	0.01629	0.55142	0.03785	16.671	1.780	0.21927	0.01614	2831.1	159.2	2975.3	123.9	95.2	4.8	5.45	62	77	66	0.68
D-36.1	950	694	0.76	688	64	0.00013	0.00001	0.00173	0.20805	0.02266	0.58962	0.05966	17.884	3.045	0.21998	0.02747	2987.9	246.6	2980.6	216.8	100.2	-0.2	15.09	59	81	69	0.75
D-25.1	716	271	0.39	462	40	0.00012	0.00016	0.00150	0.10854	0.01187	0.56472	0.05424	17.153	2.828	0.22029	0.02699	2886.1	227.5	2982.8	212.4	96.8	3.2	10.77	52	83	65	0.79
D-13.1†	300	175	0.60	194	218	0.00153	0.00009	0.01987	0.16551	0.01479	0.54196	0.02422	16.547	1.234	0.22144	0.01204	2791.6	102.1	2991.2	90.3	93.3	6.7	4.69	73	120	92	0.72
D-1.1	479	339	0.73	366	2	0.00001	0.00005	0.00013	0.24285	0.01388	0.60565	0.03654	18.582	1.995	0.22252	0.01815	3052.5	148.4	2999.1	137.6	101.8	-1.8	7.66	82	107	89	0.72
D-55.1	506	387	0.79	355	7	0.00003	0.00003	0.00038	0.21604	0.00896	0.56433	0.02879	17.475	1.214	0.22459	0.00924	2884.5	119.8	3013.9	67.7	95.7	4.3	8.22	85	100	89	0.79
D-42.1†	182	125	0.71	88	124	0.00194	0.00150	0.02482	0.16359	0.04981	0.40094	0.01211	12.873	1.352	0.23286	0.02256	2173.4	56.0	3071.8	163.9	70.8	29.2	3.01	68	84	72	0.82
D-17.1†	150	83	0.57	99	192	0.00259	0.00067	0.03299	0.14482	0.02520	0.55789	0.01059	18.139	0.975	0.23581	0.01131	2857.9	44.0	3091.9	78.7	92.4	7.6	2.45	87	123	100	0.74
D-7.1†	100	75	0.78	73	20	0.00041	0.00038	0.00515	0.22088	0.02112	0.58139	0.02424	19.310	1.465	0.24089	0.01406	2954.4	99.6	3125.9	96.0	94.5	5.5	1.71	56	135	85	0.63
D-40.1	294	206	0.73	228	7	0.00004	0.00005	0.00055	0.18733	0.00298	0.62939	0.01514	21.441	0.537	0.24707	0.00113	3147.2	60.2	3166.1	7.3	99.4	0.6	5.09	69	94	78	0.77
D-14.1	126	48	0.39	91	11	0.00016	0.00052	0.00197	0.10985	0.01789	0.61833	0.01880	21.180	1.097	0.24843	0.00952	3103.3	75.3	3174.8	62.1	97.7	2.3	2.09	80	137	104	0.74
D-56.1	169	114	0.70	126	38	0.00042	0.00004	0.00531	0.17211	0.00520	0.61121	0.01126	21.041	0.461	0.24967	0.00243	3074.9	45.2	3182.7	15.5	96.6	3.4	2.94	70	93	80	0.73
D-51.1	176	96	0.56	139	15	0.00015	0.00063	0.00192	0.13757	0.02123	0.65837	0.02331	22.866	1.424	0.25189	0.01183	3260.8	91.2	3196.7	76.3	102.0	-2.0	3.03	66	132	92	0.71
D-43.1	1493	609	0.42	1171	285	0.00033	0.00018	0.00414	0.11066	0.00650	0.66502	0.01633	23.803	0.819	0.25959	0.00550	3286.6	63.6	3244.3	33.8	101.3	-1.3	25.73	59	108	78	0.75
D-32.1	449	114	0.26	336	124	0.00049	0.00021	0.00605	0.06654	0.01143	0.65379	0.02747	23.724	1.770	0.26318	0.01490	3243.0	108.0	3265.8	92.0	99.3	0.7	7.62	67	90	75	0.83
D-39.1†	433	418	1.00	328	206	0.00091	0.00025	0.01123	0.20108	0.02326	0.59927	0.05806	22.208	3.277	0.26877	0.02684	3026.9	238.4	3298.9	166.2	91.8	8.2	8.33	75	102	83	0.78
D-26.1†	321	25	0.08	204	595	0.00363	0.00030	0.04435	0.02341	0.01134	0.56820	0.02402	21.491	1.540	0.27432	0.01449	2900.4	99.5	3330.9	85.2	87.1	12.9	5.48	50	107	74	0.67
D-27.1†	627	107	0.18	424	102	0.00031	0.00103	0.00381	0.02265	0.03296	0.60599	0.13806	22.997	5.559	0.27524	0.01573	3053.9	579.4	3336.1	92.4	91.5	8.5	10.89	39	67	48	0.57
D-31.1†	736	203	0.29	550	285	0.00070	0.00005	0.00850	0.07721	0.00488	0.63991	0.03194	24.649	1.807	0.27936	0.01335	3188.7	126.8	3359.4	76.7	94.9	5.1	13.15	81	111	92	0.73
D-28.1†	725	360	0.51	550	131	0.00034	0.00002	0.00410	0.14618	0.00103	0.61548	0.01163	24.150	0.492	0.28458	0.00159	3091.9	46.6	3388.2	8.7	91.3	8.7	13.60	53	93	66	0.74
D-41.1†	1049	450	0.44	587	307	0.00073	0.00002	0.00871	0.10532	0.00445	0.46624	0.01738	18.643	1.059	0.29000	0.01115	2467.1	76.9	3417.6	61.1	72.2	27.8	19.76	71	135	99	0.74
D-29.1†	216	106	0.51	154	32	0.00030	0.00004	0.00358	0.13167	0.00177	0.57808	0.05307	23.526	3.317	0.29515	0.02838	2940.9	220.5	3445.0	157.8	85.4	14.6	4.17	50	107	72	0.70
D-60.1	778	56	0.07	607	89	0.00019	0.00007	0.00232	0.02129	0.00258	0.68842	0.02888	28.024	1.900	0.29524	0.01425	3376.6	111.2	3445.5	77.0	98.0	2.0	14.06	82	157	111	0.68
D-8.1†	415	223	0.55	245	19	0.00011	0.00007	0.00136	0.18917	0.00387	0.46168	0.00752	19.012	0.359	0.29867	0.00232	2447.0	33.3	3463.4	12.1	70.7	29.3	8.12	75	121	90	0.26
D-22.1	538	53	0.10	448	24	0.00007	0.00002	0.00086	0.02769	0.00249	0.72768	0.04807	30.249	2.953	0.30149	0.01932	3524.8	181.9	3477.9	102.9	101.3	-1.3	9.93	76	110	85	0.72
D-44.1†	329	114	0.36	266	215	0.00113	0.00007	0.01332	0.10223	0.00399	0.66950	0.01245	28.009	0.920	0.30342	0.00754	3303.9	48.2	3487.8	39.0	94.7	5.3	6.33	55	126	85	0.69
D-52.1†	465	358	0.79	413	76	0.00028	0.00006	0.00330	0.22308	0.00394	0.67240	0.01542	28.992	0.841	0.31272	0.00473	3315.1	59.7	3534.4	23.5	93.8	6.2	9.75	78	123	92	0.74
D-11.1	480	247	0.53	436	1283	0.00411	0.00019	0.04803	0.14347	0.00691	0.72157	0.01196	31.546	0.651	0.31708	0.00331	3502.0	44.9	3555.7	16.2	98.5	1.5	9.81	61	127	84	0.35
D-61.1	144	21	0.15	125	3	0.00004	0.00034	0.00042	0.04224	0.01091	0.73878	0.01417	32.775	0.919	0.32176	0.00585	3566.0	52.7	3578.3	28.2	99.7	0.3	2.82	71	139	99	0.54
D-53.1	517	332	0.66	498	11	0.00003	0.00056	0.00040	0.17397	0.01758	0.74322	0.02051	34.178	1.377	0.33352	0.00871	3582.5	76.3	3633.3	40.6	98.6	1.4	11.16	70	132	95	0.74

Dwyer Lake Quartzite, Slave Province, Magnetic Fraction 'E' 1.0A 10°M

																	Apparent Ages (Ma)									
Spot name	U (ppm)	Th (ppm)	Th/U	Pb (ppm)	204Pb (ppb)	204Pb/ 206Pb	±204Pb/ 206Pb	f206	208Pb/ 206Pb	±208Pb/ 206Pb	206Pb/ 238U	±206Pb/ 238U	207Pb/ 235U	±207Pb/ 235U	207Pb/ 206Pb	±207Pb/ 206Pb	206Pb/ 238U	±206Pb/ 238U	207Pb/ 206Pb	±207Pb/ 206Pb	Conc.%	Disc.%	a-dose events/mg x 10^15	Breadth µm	Length µm	EqDiam µm	Form Factor
E-14.1†§	1199	313	0.27	181	32	0.00023	0.00022	0.00313	0.10480	0.01276	0.13635	0.01243	3.381	0.486	0.17982	0.01806	824.0	70.9	2651.2	177.1	31.1	68.9	14.86	66	129	91	0.68
E-70.1†§	2236	160	0.07	633	259	0.00049	0.00015	0.00671	0.02029	0.00538	0.27285	0.00496	6.996	0.174	0.18595	0.00278	1555.3	25.2	2706.6	24.9	57.5	42.5	27.60	94	123	102	0.80
E-50.1§	1255	347	0.29	719	125	0.00022	0.00003	0.00302	0.09349	0.00204	0.51646	0.01251	13.889	0.451	0.19504	0.00368	2684.2	53.4	2785.2	31.2	96.4	3.6	16.75	78	117	94	0.70
E-55.1§	1304	529	0.42	774	31	0.00005	0.00001	0.00070	0.10939	0.01905	0.52854	0.05738	14.244	2.311	0.19546	0.02106	2735.3	246.6	2788.7	188.3	98.1	1.9	17.82	73	99	84	0.76
E-60.1†§	1037	1193	1.19	493	81	0.00025	0.00062	0.00336	0.31763	0.02090	0.36401	0.00706	9.879	0.543	0.19683	0.00986	2001.2	33.5	2800.1	82.6	71.5	28.5	16.04	72	113	90	0.69
E-26.1†§	1425	399	0.29	710	60	0.00011	0.00003	0.00145	0.06801	0.00363	0.45712	0.02134	12.515	0.918	0.19856	0.01014	2426.8	95.1	2814.4	86.0	86.2	13.8	19.32	75	93	81	0.83
E-11.1§	1617	1232	0.79	1036	91	0.00012	0.00001	0.00167	0.20951	0.00062	0.52757	0.00937	14.589	0.266	0.20056	0.00048	2731.2	39.7	2830.8	3.9	96.5	3.5	23.94	71	103	86	0.73
E-40.1†	711	672	0.98	426	48	0.00016	0.00001	0.00219	0.25729	0.01534	0.47593	0.00943	13.470	0.379	0.20527	0.00363	2509.5	41.3	2868.6	29.0	87.5	12.5	11.03	60	104	77	0.71
E-31.1	1116	610	0.56	695	23	0.00004	0.00001	0.00059	0.15498	0.00409	0.53172	0.01194	15.109	0.530	0.20609	0.00501	2748.7	50.5	2875.0	40.0	95.6	4.4	16.32	62	80	65	0.60
E-64.1†	649	262	0.42	309	276	0.00116	0.00068	0.01540	0.10997	0.02295	0.41973	0.01666	11.992	1.061	0.20721	0.01538	2259.3	76.1	2883.8	126.0	78.3	21.7	9.31	71	120	90	0.53
E-13.1†	1098	465	0.44	273	40	0.00020	0.00004	0.00259	0.12292	0.00464	0.21732	0.00939	6.211	0.490	0.20727	0.01262	1267.7	49.9	2884.3	102.5	44.0	56.0	15.81	64	123	87	0.58
E-53.1	1354	540	0.41	902	53	0.00008	0.00001	0.00104	0.11702	0.00871	0.58377	0.01836	16.775	0.647	0.20841	0.00390	2964.1	75.2	2893.2	30.7	102.4	-2.4	19.51	68	98	80	0.72
E-21.1†	2159	765	0.37	522	2952	0.00663	0.00018	0.08760	0.07217	0.07436	0.21950	0.01241	6.335	0.482	0.20933	0.00926	1279.2	65.9	2900.3	73.6	44.1	55.9	30.99	76	126	95	0.61
E-61.1†	748	602	0.83	490	11	0.00003	0.00002	0.00044	0.22503	0.01021	0.53032	0.00986	15.312	0.323	0.20940	0.00165	2742.8	41.7	2900.9	12.8	94.5	5.5	11.56	78	110	90	0.72
E-54.2R	932	372	0.41	568	69	0.00016	0.00013	0.00213	0.11017	0.01348	0.53576	0.02619	15.551	1.237	0.21052	0.01198	2765.7	110.9	2909.6	95.3	95.1	4.9	13.55	*	*	*	*
E-34.1	897	415	0.48	574	150	0.00035	0.00005	0.00464	0.13632	0.00406	0.55146	0.01033	16.067	0.480	0.21131	0.00445	2831.3	43.1	2915.6	34.5	97.1	2.9	13.21	69	102	82	0.73
E-9.1	965	392	0.42	592	184	0.00041	0.00003	0.00539	0.10895	0.00504	0.53991	0.01392	15.761	0.667	0.21172	0.00645	2783.1	58.5	2918.7	50.2	95.4	4.6	14.11	71	100	83	0.75
E-43.1†	1223	640	0.54	675	737	0.00149	0.00070	0.01953	0.17008	0.02994	0.46390	0.01833	13.556	2.046	0.21194	0.02985	2456.8	81.2	2920.5	248.4	84.1	15.9	18.24	68	117	92	0.73
E-12.1	969	394	0.42	598	841	0.00182	0.00021	0.02390	0.10651	0.00707	0.54336	0.01045	15.902	0.510	0.21226	0.00496	2797.5	43.8	2922.9	38.4	95.7	4.3	14.20	66	103	82	0.80
E-38.1†	716	519	0.75	413	1072	0.00350	0.00006	0.04595	0.19235	0.02209	0.47697	0.01162	13.964	1.183	0.21233	0.01659	2514.1	50.9	2923.4	132.4	86.0	14.0	11.04	62	98	77	0.80
E-22.1	833	887	1.10	607	9	0.00002	0.00007	0.00029	0.29746	0.01759	0.56034	0.00920	16.450	0.363	0.21291	0.00274	2868.1	38.1	2927.8	21.0	98.0	2.0	13.56	70	108	85	0.72
E-44.1†	871	176	0.21	459	912	0.00245	0.00036	0.03221	0.05684	0.01365	0.48205	0.01074	14.163	0.835	0.21309	0.01106	2536.2	46.9	2929.2	86.5	86.6	13.4	12.37	69	90	76	0.75
E-32.1†	482	351	0.75	275	37	0.00018	0.00021	0.00239	0.12758	0.01556	0.49324	0.02061	14.528	0.799	0.21362	0.00660	2584.7	89.6	2933.2	50.8	88.1	11.9	7.48	73	120	88	0.71
E-41.1	609	280	0.47	405	50	0.00016	0.00029	0.00216	0.12754	0.01087	0.57655	0.01019	16.994	0.890	0.21378	0.01008	2934.7	41.8	2934.4	78.3	100.0	0.0	9.05	80	103	87	0.77
E-56.1	664	291	0.45	439	38	0.00012	0.00013	0.00151	0.13017	0.00541	0.57198	0.01719	16.874	0.740	0.21397	0.00608	2916.0	70.9	2935.8	46.7	99.3	0.7	9.84	70	130	97	0.37
E-29.1	489	260	0.55	319	3	0.00001	0.00004	0.00019	0.15501	0.00230	0.55230	0.03279	16.353	1.304	0.21474	0.00995	2834.7	137.7	2941.7	76.9	96.4	3.6	7.39	51	102	69	0.64
E-75.1	603	309	0.53	401	30	0.00010	0.00005	0.00135	0.13837	0.00177	0.57154	0.01038	16.968	0.325	0.21532	0.00091	2914.1	42.7	2946.0	6.9	98.9	1.1	9.09	108	137	118	0.75
E-73.1	712	526	0.76	499	7	0.00002	0.00008	0.00026	0.21455	0.01398	0.56925	0.03738	16.910	1.644	0.21545	0.01379	2904.7	155.4	2947.0	107.3	98.6	1.4	11.13	77	128	94	0.73
E-18.1	789	585	0.77	570	18	0.00004	0.00011	0.00058	0.20847	0.02181	0.58923	0.06105	17.574	2.722	0.21632	0.02226	2986.3	252.5	2953.5	176.6	101.1	-1.1	12.39	67	108	81	0.70
E-17.1	447	227	0.52	307	4	0.00002	0.00012	0.00025	0.14361	0.00449	0.58650	0.00974	17.538	0.370	0.21687	0.00241	2975.2	39.7	2957.6	18.0	100.6	-0.6	6.77	57	94	71	0.66
E-68.1†	504	275	0.56	278	787	0.00344	0.00035	0.04487	0.04743	0.01845	0.50681	0.04644	15.211	2.407	0.21767	0.02570	2643.0	201.8	2963.6	204.4	89.2	10.8	7.71	74	109	84	0.75
E-54.1†	263	156	0.61	159	4	0.00004	0.00006	0.00050	0.17388	0.00197	0.50367	0.01091	15.132	0.360	0.21790	0.00162	2629.6	47.0	2965.2	12.0	88.7	11.3	4.06	79	154	110	0.68
E-52.1	1055	345	0.34	704	3661	0.00635	0.00049	0.08292	0.10728	0.02760	0.58486	0.04268	17.609	2.400	0.21836	0.02323	2968.6	176.0	2968.7	182.7	100.0	0.0	15.61	77	137	104	0.12
E-2.1	457	305	0.69	315	11	0.00005	0.00004	0.00064	0.18679	0.00431	0.56953	0.00964	17.157	0.385	0.21848	0.00279	2905.9	39.7	2969.5	20.8	97.9	2.1	7.15	53	108	68	0.57
E-33.1	1208	103	0.09	759	10	0.00002	0.00001	0.00021	0.02355	0.00160	0.58823	0.03793	17.727	1.704	0.21857	0.01392	2982.2	155.8	2970.2	106.5	100.4	-0.4	17.17	61	91	71	0.69
E-8.1	917	472	0.53	629	10	0.00002	0.00055	0.00029	0.14245	0.02123	0.58488	0.04388	17.634	2.051	0.21866	0.01750	2968.7	181.0	2970.9	135.2	99.9	0.1	14.01	96	131	110	0.77
E-4.1	273	109	0.41	180	249	0.00180	0.00009	0.02352	0.11116	0.03978	0.57709	0.01084	17.440	0.375	0.21919	0.00184	2936.9	44.5	2974.7	13.6	98.7	1.3	4.10	56	129	84	0.65
E-10.1	468	260	0.57	320	13	0.00006	0.00004	0.00072	0.15082	0.00312	0.57764	0.01291	17.798	0.570	0.22347	0.00454	2939.1	53.0	3005.9	33.0	97.8	2.2	7.33	78	147	106	0.76
E-47.1†	898	125	0.14	345	1465	0.00498	0.00006	0.06459	0.02790	0.00298	0.35715	0.02320	11.028	0.737	0.22395	0.00215	1968.6	111.2	3009.3	15.5	65.4	34.6	13.15	65	98	77	0.30
E-58.1	997	319	0.33	635	27	0.00006	0.00014	0.00073	0.09000	0.00756	0.56351	0.01807	17.420	0.803	0.22420	0.00658	2881.1	75.0	3011.1	47.9	95.7	4.3	15.06	72	108	87	0.48
E-27.1†	713	630	0.91	341	187	0.00077	0.00067	0.00987	0.18751	0.02215	0.39044	0.00734	12.763	0.630	0.23708	0.01028	2124.9	34.1	3100.5	70.8	68.5	31.5	12.31	60	81	68	0.82
E-3.1	297	179	0.62	224	10	0.00006	0.00004	0.00082	0.17431	0.00782	0.61794	0.02358	20.938	1.102	0.24575	0.00781	3101.7	94.7	3157.6	51.3	98.2	1.8	5.05	72	94	80	0.77
E-62.1†	828	510	0.64	576	659	0.00160	0.00006	0.02013	0.17162	0.00356	0.56981	0.00923	19.360	0.355	0.24642	0.00167	2907.0	38.0	3161.9	10.8	91.9	8.1	14.14	77	99	85	0.79
E-72.1	633	342	0.56	495	34	0.00010	0.00001	0.00120	0.14611	0.00310	0.65189	0.01232	22.211	1.871	0.24711	0.01971	3235.6	48.3	3166.4	132.5	102.2	-2.2	10.70	47	101	66	0.65
E-24.1	484	296	0.63	377	7	0.00003	0.00002	0.00035	0.15980	0.00628	0.64419	0.01723	21.958	1.263	0.24722	0.01179	3205.5	67.9	3167.1	77.7	101.2	-1.2	8.28	56	87	66	0.46
E-48.1	585	621	1.10	516	139	0.00042	0.00001	0.00524	0.29550	0.00233	0.66268	0.03195	22.731	2.505	0.24878	0.02320	3277.6	125.1	3177.0	156.1	103.2	-3.2	10.77	76	108	87	0.55
E-19.1	693	642	0.96	557	174	0.00047	0.00040	0.00589	0.25502	0.01341	0.61993	0.01386	21.294	0.750	0.24913	0.00613	3109.6	55.4	3179.2	39.5	97.8	2.2	12.52	69	122	90	0.75
E-36.1†	355	225	0.65	256	31	0.00018	0.00017	0.00221	0.18047	0.00994	0.58665	0.00953	20.195	0.417	0.24967	0.00272	2975.8	38.8	3182.7	17.4	93.5	6.5	6.14	69	81	74	0.78
E-51.1†	955	333	0.36	637	312	0.00066	0.00008	0.00823	0.09528	0.00938	0.57528	0.04540	19.949	2.401	0.25149	0.02050	2929.5	188.5	3194.2	135.3	91.7	8.3	15.90	68	101	82	0.78
E-42.1	239	168	0.73	182	2	0.00002	0.00002	0.00022	0.16940	0.04092	0.62155	0.05645	22.028	2.973	0.25703	0.02291	3116.1	228.4	3228.6	148.2	96.5	3.5	4.27	68	95	78	0.77
E-46.1†	420	199	0.49	282	4021	0.01599	0.00036	0.20037	0.13977	0.01696	0.55929	0.01502	19.841	0.941	0.25728	0.00923	2863.7	62.4	3230.2	57.8	88.7	11.3	7.25	68	102	80	0.56
E-74.1	729	424	0.60	575	10	0.00002	0.00000	0.00029	0.15788	0.00442	0.64403	0.02248	23.479	1.087	0.26441	0.00698	3204.8	88.7	3273.2	42.1	97.9	2.1	13.09	81	124	100	0.70
E-69.1†	1016	319	0.32	646	13	0.00003	0.00016	0.00033	0.05408	0.00540	0.56009	0.01804	20.436	0.760	0.26463	0.00397	2867.0	75.0	3274.5	23.8	87.6	12.4	17.52	69	134	92	0.71
E-20.1	923	161	0.18	677	15	0.00003	0.00001	0.00035	0.04567	0.00499	0.64901	0.07056	23.985	3.870	0.26803	0.02853	3224.4	281.9	3294.5	177.9	97.9	2.1	15.72	78	108	86	0.68
E-49.1†	427	174	0.42	233	2351	0.01229	0.00095	0.15195	0.15889	0.05204	0.44291	0.03482	16.378	2.909	0.26819	0.04015	2363.7	157.5	3295.5	257.2	71.7	28.3	7.56	62	95	75	0.76
E-59.1†	937	122	0.13	648	482	0.00096	0.00060	0.01176	0.02927	0.01992	0.61896	0.03044	22.958	1.876	0.26901	0.01597	3105.8	122.4	3300.3	96.4	94.1	5.9	15.88	80	109	90	0.71
E-45.1†	435	171	0.41	266	2370	0.01075	0.00232	0.13238	0.11548	0.08293	0.51344	0.03159	19.192	3.257	0.27110	0.04085	2671.3	136.0	3312.4	258.6	80.6	19.4	7.73	88	128	105	0.72
E-7.1†	643	332	0.53	359	448	0.00173	0.00023	0.02114	0.13571	0.00811	0.46000	0.00992	17.311	0.532	0.27294	0.00529	2439.6	44.0	3323.0	30.7	73.4	26.6	11.72	81	129	103	0.71
E-5.1†	657	570	0.90	522	49	0.00015	0.00002	0.00178	0.26017	0.01019	0.60155	0.03036	22.642	1.530	0.27298	0.01067	3036.1	123.4	3323.2	62.6	91.4	8.6	12.62	65	100	79	0.70
E-35.1	742	48	0.07	539	22	0.00005	0.00001	0.00066	0.01752	0.00027	0.65333	0.01453	24.840	0.620	0.27575	0.00245	3241.2	56.9	3339.0	13.9	97.1	2.9	12.68	80	98	83	0.71
E-6.1	691	112	0.17	522	24	0.00006	0.00001	0.00075	0.04045	0.01835	0.66598	0.01395	25.641	0.641	0.27924	0.00315	3290.3	54.2	3358.7	17.7	98.0	2.0	12.12	123	191	149	0.53
E-23.1	909	21	0.02	674	8	0.00001	0.00002	0.00018	0.00606	0.00087	0.67070	0.01329	25.863	0.576	0.27967	0.00223	3308.6	51.5	3361.1	12.5	98.4	1.6	15.62	90	165	115	0.66
E-16.1	768	345	0.46	621	14	0.00003	0.00008	0.00038	0.12213	0.00654	0.66884	0.02489	26.057	1.546	0.28255	0.01180	3301.4	96.9	3377.1	66.7	97.8	2.2	14.23	52	71	59	0.77
E-25.1	815	63	0.08	636	1	0.00000	0.00007	0.00003	0.02119	0.00312	0.68859	0.05001	28.070	3.156	0.29566	0.02283	3377.2	193.8	3447.6	125.3	98.0	2.0	14.75	82	111	93	0.82
E-67.1†	390	291	0.77	308	510	0.00238	0.00034	0.02833	0.17515	0.01606	0.62332	0.02941	25.760	1.387	0.29974	0.00621	3123.1	117.9	3468.9	32.5	90.0	10.0	7.89	56	107	78	0.69
E-63.1†	833	98	0.12	521	1315	0.00323	0.00016	0.03820	0.01859	0.00697	0.54888	0.02355	23.109	1.502	0.30536	0.01337	2820.5	98.8	3497.6	69.4	80.6	19.4	15.57	61	118	82	0.70
E-66.1†	277	195	0.73	168	28	0.00024	0.00003	0.00282	0.15255	0.03095	0.48461	0.03982	20.441	3.680	0.30592	0.04596	2547.3	175.3	3500.5	254.0	72.8	27.2	5.66	88	103	88	0.65
E-30.1	518	141	0.28	422	140	0.00045	0.00003	0.00533	0.05816	0.00144	0.69093	0.01187	29.686	0.560	0.31161	0.00185	3386.2	45.4	3528.9	9.2	96.0	4.0	10.06	68	86	71	0.68
E-71.1	308	256	0.86	294	4	0.00002	0.00011	0.00025	0.22076	0.00632	0.72237	0.02396	31.446	1.127	0.31572	0.00318	3504.9	90.3	3549.1	15.6	98.8	1.2	6.56	87	143	107	0.73
E-39.1†	599	403	0.69	482	372	0.00117	0.00025	0.01365	0.20961	0.01304	0.61113	0.01758	26.854	1.242	0.31870	0.01045	3074.5	70.7	3563.6	51.4	86.3	13.7	12.56	57	108	78	0.73
E-65.1†	800	68	0.09	637	775	0.00162	0.00039	0.01878	0.02604	0.02257	0.68381	0.16259	30.750	11.488	0.32615	0.08479	3359.0	654.6	3599.1	470.1	93.3	6.7	15.66	70	109	84	0.60
E-57.1†	533	447	0.87	370	503	0.00199	0.00014	0.02303	0.16337	0.01251	0.54153	0.03896	24.407	2.557	0.32688	0.02213	2789.9	165.0	3602.5	108.0	77.4	22.6	11.66	69	82	70	0.71
E-37.1†	255	143	0.58	208	522	0.00348	0.00113	0.04005	0.10268	0.03636	0.66071	0.01490	30.361	1.733	0.33327	0.01656	3269.9	58.1	3632.2	78.3	90.0	10.0	5.44	71	119	88	0.74
E-1.1†	466	467	1.03	411	3	0.00001	0.00012	0.00011	0.25235	0.03296	0.64505	0.01307	29.854	0.779	0.33567	0.00473	3208.8	51.4	3643.2	21.7	88.1	11.9	10.64	61	97	74	0.76
E-28.1†	692	221	0.33	439	8702	0.02255	0.00108	0.25210	0.12532	0.03900	0.48661	0.01112	26.065	1.962	0.38848	0.02677	2556.0	48.4	3865.1	108.0	66.1	33.9	16.02	85	135	105	0.71
E-15.1	554	236	0.44	557	287	0.00077	0.00008	0.00840	0.10929	0.00891	0.77522	0.01528	42.323	0.967	0.39596	0.00372	3699.8	55.7	3893.8	14.2	95.0	5.0	13.22	85	130	107	0.78